AD_____

Award Number: DAMD17-03-1-0763

TITLE: Measles Virus Nucleocapsid (MVNP) Gene Expression and RANK Receptor Signaling in Osteoclast Precursors, Osteoclast Inhibitors Peptide Therapy for Pagets Disease

PRINCIPAL INVESTIGATOR: Sakamuri V. Reddy, Ph.D.

CONTRACTING ORGANIZATION: Medical University of South Carolina
Charleston, SC 29425

REPORT DATE: October 2007

TYPE OF REPORT: Annual

PREPARED FOR: U.S. Army Medical Research and Materiel Command
Fort Detrick, Maryland 21702-5012

REPORT DOCUMENTATION PAGE

Form Approved
OMB No. 0704-0188

1. REPORT DATE	2. REPORT TYPE	3. DATES COVERED
01-10-2007	Annual	24 Sep 2006 – 23 Sep 2007

4. TITLE AND SUBTITLE
Measles Virus Nucleocapsid (MVNP) Gene Expression and RANK Receptor Signaling in Osteoclast Precursors, Osteoclast Inhibitors Peptide Therapy for Pagets Disease

5a. CONTRACT NUMBER

5b. GRANT NUMBER
DAMD17-03-1-0763

5c. PROGRAM ELEMENT NUMBER

6. AUTHOR(S)

Sakamuri V. Reddy, Ph.D.

Email: reddysv@musc.edu

5d. PROJECT NUMBER

5e. TASK NUMBER

5f. WORK UNIT NUMBER

7. PERFORMING ORGANIZATION NAME(S) AND ADDRESS(ES)

Medical University of South Carolina
Charleston, SC 29425

8. PERFORMING ORGANIZATION REPORT NUMBER

9. SPONSORING / MONITORING AGENCY NAME(S) AND ADDRESS(ES)
U.S. Army Medical Research and Materiel Command
Fort Detrick, Maryland 21702-5012

10. SPONSOR/MONITOR'S ACRONYM(S)

11. SPONSOR/MONITOR'S REPORT NUMBER(S)

12. DISTRIBUTION / AVAILABILITY STATEMENT
Approved for Public Release; Distribution Unlimited

13. SUPPLEMENTARY NOTES

14. ABSTRACT

Paget's disease (PD) of bone occurs in 3-4% of population over the age of 50. We have identified expression of measles virus nucleocapsid transcripts in osteoclast (OCL) precursors and that MVNP expression induces pagetic phenotype in osteoclasts with increased bone resorption activity as seen in patients with Paget's disease. We previously cloned and identified osteoclast inhibitory peptide-1 (OIP-1/hSca) which inhibits osteoclast formation and bone resorption. We hypothesize that MVNP expression in osteoclast precursors modulates RANK receptor signaling leading to Pagetic OCL development. OIP-1 blocks these signaling events and inhibits MVNP induced osteoclastogenesis and elevated bone resorption activity. We demonstrated that MVNP increases TNF-alpha induced OCL differentiation and activation by increasing NF-kB signaling through increased expression of p62, and IKK-gama and increased MAPK signaling. Our results also suggest that MVNP's effects on TNF-alpha signaling contribute to the increased OCL formation in PD. Furthermore, expression of MVNP gene in OCL in vivo induces a pagetic-like phenotype. RANKL stimulation of OIP-1 mice derived bone marrow cells resulted in significantly decreased osteoclast formation. Furthermore, OIP-1 transgenic mouse bones demonstrated an osteopetrotic phenotype. These data suggest that OIP-1 is an important physiologic regulator of osteoclast development and bone resorption in vivo and may have therapeutic utility to control excess bone turnover in patients with Paget's disease.

15. SUBJECT TERMS
Not Provided

16. SECURITY CLASSIFICATION OF:			17. LIMITATION OF ABSTRACT	18. NUMBER OF PAGES	19a. NAME OF RESPONSIBLE PERSON
a. REPORT	b. ABSTRACT	c. THIS PAGE			USAMRMC
U	U	U	UU	27	19b. TELEPHONE NUMBER *(include area code)*

Standard Form 298 (Rev. 8-98)
Prescribed by ANSI Std. Z39.18

Table of Contents

–

INTRODUCTION:

Paget's disease affects approximately 2-3 million people in the United States and is the second most common bone disease after osteoporosis. We shown that bone marrow cells from patients with Paget's disease express measles virus nucleocapsid protein (MVNP) transcripts and further demonstrated that expression of the Edmonston MVNP gene in normal osteoclast (OCL) precursors results in formation of OCL that share many of the characteristics of OCL from Paget's patients. The MVNP gene contained several sense mutations, which constituted 1% of the nucleotide sequence. The pathologic significance of MVNP and associated mutations to induce abnormal OCL formation and activity in Paget's disease, is unknown (1). RANKL is a member of Tumor necrosis factor (TNF) family member that is expressed on stromal/osteoblast cells and RANK receptor is expressed on committed osteoclast precursor cells. RANKL/RANK signaling is critical for osteoclast differentiation and bone resorption activity in vitro and in vivo (2,3). We have recently cloned and identified the Ly-6 family member, osteoclast inhibitory peptide-1 (OIP-1/hSca) which inhibits osteoclast formation and bone resorption activity. We have further demonstrated that OIP-1 significantly inhibits TNF receptor associated factor-2 (TRAF-2) and c-Jun kinase activity in osteoclast precursor cells (4). Our hypothesis is that MVNP expression in osteoclast precursors modulates the status of RANK receptor signaling molecules leading to Pagetic OCL development in Paget's disease. OIP-1 blocks RANK receptor signaling events and inhibits MVNP induced osteoclastogenesis and elevated bone resorption activity in Paget's patients.

BODY:

The progress on Task-3 (35-45 months) in the statement of work is as follow:

Task 1. Determine the sensitivity of MVNP transduced osteoclast precursors to RANK Ligand (RANKL) and TNF-alpha stimulation to form pagetic osteoclasts (Months 1-24):

Completed

Task 2. Determine the RANK receptor signaling in MVNP transduced osteoclast precursors (Months 24-36).

Completed

Task 3. Determine the effects of OIP-1 on MVNP altered RANK receptor signaling in osteoclast precursor cells (Months 29-48).

(a) Determine the effect of OIP-1 on osteoclast differentiation of MVNP transduced osteoclast precursors (Months 29-35).

Completed

(b) Assess the status of RANK receptor signaling molecules in MVNP stimulated osteoclasts (35-41).

Mutations in the sequestosome 1 (p62) gene has been reported in patients with Paget's disease. In previous report, we have shown that a mutant p62 (*P392L*) modulates NF-kB signaling during osteoclast (OCL) differentiation. We further identified that both wild-type *p62* and mutant *p62P392L* transduced OCL precursors formed significantly larger osteoclasts compared to empty vector (EV) transduced cells (Fig.1). However, our results concluded that mutation of the *p62* gene increases osteoclastogenesis but do not induce Paget disease (article appended).

In the present study period, we have characterized transgenic mice targeted with osteoclast inhibitory peptide-1 (OIP-1) expression to the cells of osteoclast linage using the mouse tartrate resistant acid phosphatase gene promoter. The OIP-1 mice demonstrated osteopetrotic bone phenotype (article appended). We have performed ex vivo experiments using bone marrow cells isolated from the OIP-1 and wild-type mice to further assess OIP-1 inhibition of OCL formation. Non-adherent bone marrow cells derived from the wild-type and OIP-1 mice were cultured in the presence of hGM-CSF (10 ng/ml) in methyl cellulose (1.2%) to form CFU-GM colonies. As shown in Fig.2A, OIP-1 transgenic mouse lines #5 and #13 derived cells showed a significant decrease in the number of CFU-GM colonies by 35% and 41% respectively, compared to control mice. We further examined the capacity for OCL differentiation and bone resorption by OIP-1 transgenic mouse derived bone marrow cells. OIP-1 and wild-type mice derived non-adherent bone marrow cells were stimulated with various concentrations of RANKL (5-100 ng/ml) with M-CSF (10 ng/ml), and the number of TRAP positive multinucleated OCLs formed in these cultures were scored. As shown in Fig.2B, the number of OCLs formed in OIP-1 #5 and OIP-1 #13 mouse bone marrow cultures was significantly decreased by 39% and 42% respectively, compared to control mice in response to RANKL (100 ng/ml) treatment. We further examined the effects of MVNP on RANK-RANKL signaling in wild-type and OIP-1 transgenic mice derived preosteoclast cells. The non-adherent bone marrow cells from wild-type and OIP-1 mice were transduced with EV or MVNP and cultured with 10 ng/ml M-CSF and 100 ng/ml RANKL for 48 hours to induce osteoclast differentiation. Western blot analysis of total cel lysates obtained revealed that OIP-1 did not affect the levels of RANK receptor expression in these cells. However, there is a significant increase (2.5 fold) in the levels of RANK adaptor protein TRAF2 expression in MVNP transduced wild-type mouse preosteoclast cells, but not TRAF 6. Interestingly, OIP-1 mice derived preosteoclast cells demonstrated no significant increase in the levels of TRAF2 in response to MVNP expression. In addition, transcription factors such as c-Fos, NFATc1 critical for OCL differentiation were significantly decreased in OIP-1 transgenic mice derived preosteoclast cells compared to wild-type mice (Fig.3A). We further examined the c-Jun N-terminal kinase (JNK) activation in response to MVNP stimulation in OIP-1 mouse derived preosteoclast cells. As shown in Fig.3B, OIP-1 mouse derived preosteoclast cells transduced with MVNP showed a significant inhibition of JNK phosphorylation in response to RANKL stimulation compared to wild-type mice. Furthermore, the JNK activators such as Rac1 and ASK1 expression was also inhibited in the OIP-1 derived preosteoclast cells stimulated with MVNP when compared with wild-type mice (Fig.3C). Taken together, these results suggest that OIP-1 inhibits MVNP stimulated RANK-RANKL signaling during osteoclast differentiation.

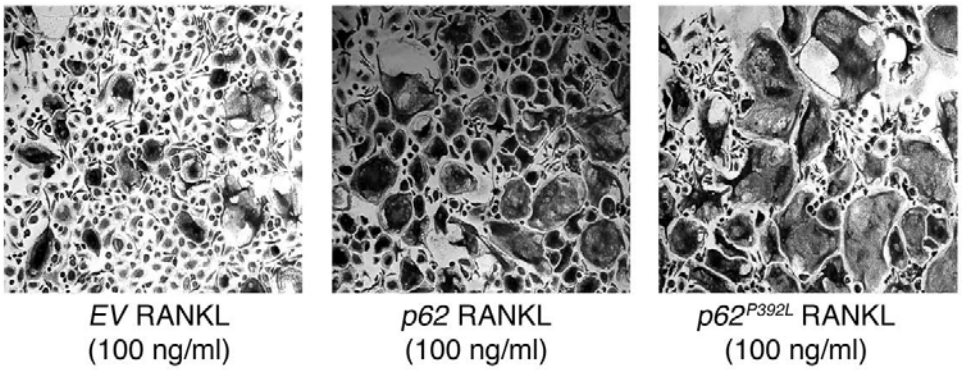

Fig.1 OCL formation by *p62* and *p62P392L* transduced human OCL precursors. GM-CFU–derived cells transduced with *p62*, *p62P392L*, or *EV* were cultured with RANKL.

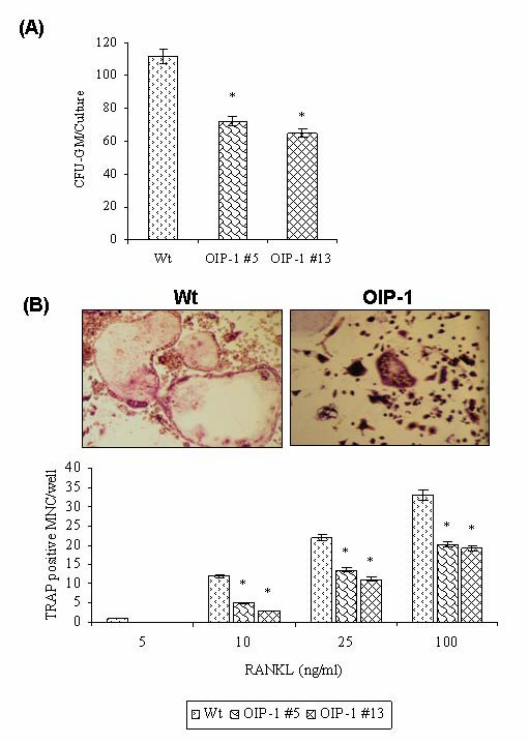

Fig.2. Inhibition of osteoclastogenesis in OIP-1 mouse bone marrow cultures. (A) CFU-GM formation in OIP-1 mouse bone marrow cultures. Wild-type (Wt) and OIP-1 mouse derived non-adherent bone marrow cells (4×10^5/ml) were cultured with hGM-CSF (10 ng/ml) in 1.2% methyl cellulose to form CFU-GM colonies. At the end of a 7 day culture period, CFU-GM colonies (aggregates >50 cells) formed in these cultures were scored using a light microscope. (B) Wild-type (Wt) and OIP-1 transgenic mouse bone marrow derived non-adherent cells were stimulated with RANKL (5-100 ng/ml) and M-CSF (10 ng/ml) for 5 days and the TRAP (+) multinucleated OCLs formed in these cultures were scored. The results represent quadruplicate cultures of three independent experiments ($p<0.05$).

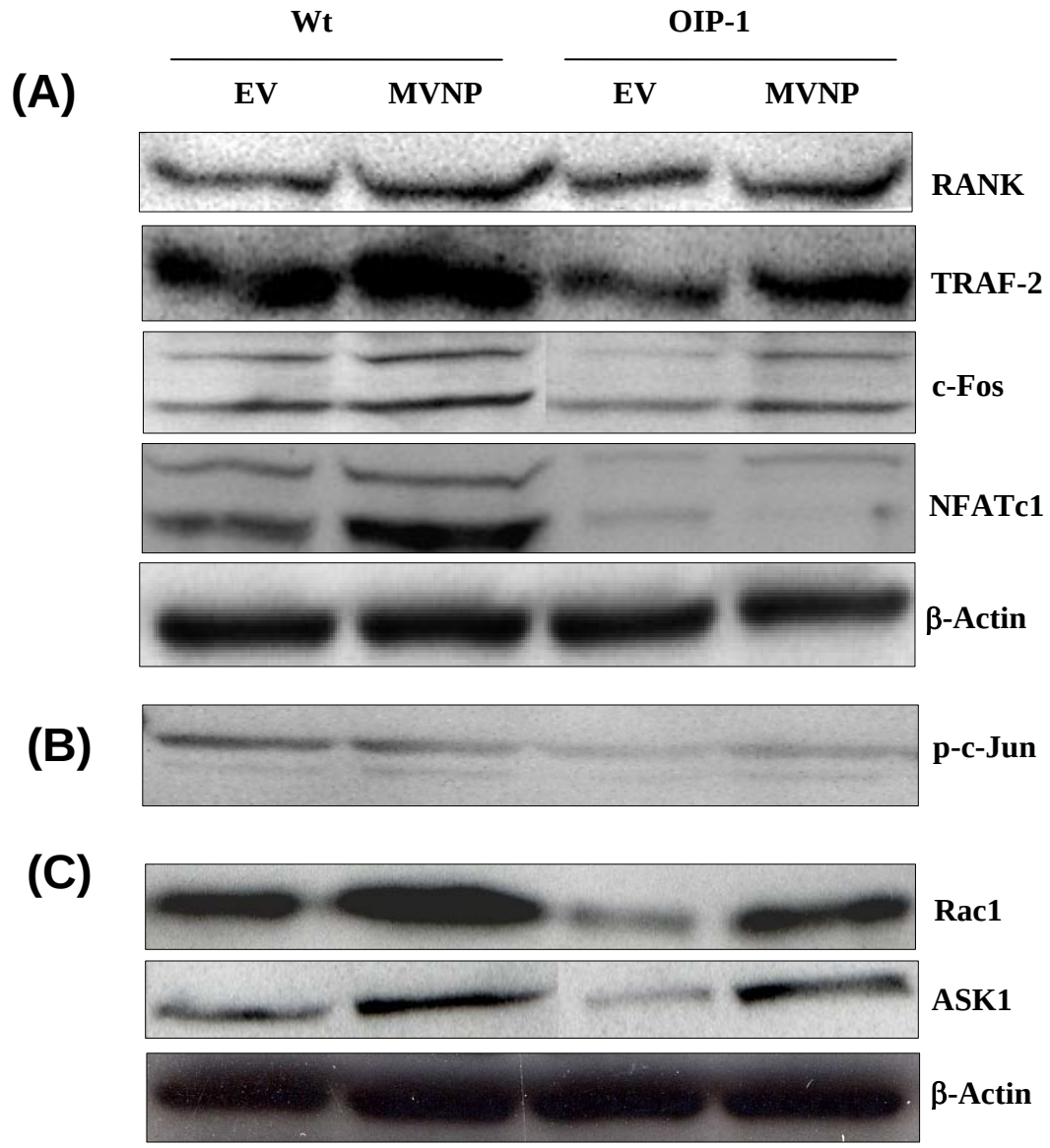

Fig.3 Western blot analysis of RANK receptor signaling molecules in wild type (Wt) and OIP-1 transgenic mice derived bone marrow cells transduced with empty vector (EV) or MVNP retrovirus. (A-C)Bone marrow cells from Wt and OIP-1 mice were transduced with MVNP or EV and cultured in presence of 10 ng/ml mMCSF and 100 ng/ml mRANKL for 2 days total cell lysates prepared were subjected to western blot analysis.

(c) Determine the potential of OIP-1 to block MVNP stimulated osteoclast formation and bone resorption in vivo (41-48).

Not yet initiated

KEY RESEARCH ACCOMPLISHMENTS:

We identified that OIP-1 expression significantly decreased MVNP enhanced levels of TRAF2, c-Fos, p-c-Jun and NFATc1. However no change in the levels of RANK and TRAF6 expression in RANKL stimulated mouse bone marrow cultures.

REPORTABLE OUTCOMES:

Published articles relevant to the proposal:

1. Kurihara N, Hiruma Y, Zhou H, Subler MA, Dempster DW, Singer, FR, **Reddy SV**, Gruber HE, Windle JJ and Roodman GD. Mutation of the sequestosome-1 gene (p62) increases osteoclastogenesis but does not induce paget disease. J Clin Invest. 117: 133–142, 2007.

2. Srinivasan S, Irie K, Key Jr, LL, Ries WL and **Reddy SV**. Transgenic mice with OIP-1/hSca over-expression targeted to the osteoclast lineage develop osteopetrosis bone phenotype. J Pathol. 2007 [Epub ahead of print].

Abstracts:

1. S. Shanmugarajan, C. Beeson, S. V. Reddy. Characterization of Osteoclast Inhibitory Peptide-1 (OIP-1/hSca) Binding to Fc Gamma Receptor II B (FcRγ) on Osteoclast Precursor Cells, ASBMR 29th Annual meeting, Hawaii, Sept. 2007.

2. K. Sundaram1, J. Senn1, D. S. Rao2, S. V. Reddy1. Enhanced Levels of FGF-2 and SOCS Signaling Modulates RANK Ligand Expression in Patients with Paget's Disease, ASBMR 29th Annual meeting, Hawaii, Sept. 2007.

CONCLUSIONS:

- In conclusion, OIP-1 inhibits MVNP stimulated Pagetic osteoclast formation/activity through suppression of RANK signaling. OIP-1 may have therapeutic utility against excess bone turnover associated with Paget's disease.

REFERENCES:

1. S.L. Teitelbaum, F.P. Ross, *Nat. Rev. Genet.* **4,** 638 (2003)
2. G. D. Roodman, Windle JJ, *J Clin Invest.* **115,** 200 (2005)
3. J.L. Roccisana *et al., J. Biol. Chem.* **279,** 10500 (2004).
4. M. Koide, H. Maeda *et al., J Bone Miner Res.* **18,** 458 (2003).

APPENDICES:

Reprints enclosed for two relevant articles as noted under outcomes.

Journal of Pathology
J Pathol (2007)
Published online in Wiley InterScience
(www.interscience.wiley.com) **DOI:** 10.1002/path.2241

Original Paper

Transgenic mice with OIP-1/hSca overexpression targeted to the osteoclast lineage develop an osteopetrosis bone phenotype

S Shanmugarajan,[1] K Irie,[2] C Musselwhite,[1] LL Key Jr,[1] WL Ries[1] and SV Reddy[1]*

[1] *Children's Research Institute, Medical University of South Carolina, Charleston, SC 29425, USA*
[2] *Department of Oral Anatomy, School of Dentistry, Health Sciences University of Hokkaido, 1757 Kanazawa, Ishikari-Tobetsu, Hokkaido 061-0293, Japan*

**Correspondence to:*
SV Reddy, Charles P Darby Children's Research Institute, 173 Ashley Avenue, Charleston, SC 29425, USA.
E-mail: reddysv@musc.edu

No conflicts of interest were declared.

Received: 26 May 2007
Revised: 5 July 2007
Accepted: 10 August 2007

Abstract

Regulatory mechanisms operative in bone-resorbing osteoclasts are complex. We previously defined the *Ly-6* gene family member OIP-1/hSca as an inhibitor of osteoclastogenesis *in vitro*; however, a role in skeletal development is unknown. In this study, we developed transgenic mice with OIP-1/hSca expression targeted to the osteoclast lineage that develop an osteopetrotic bone phenotype. Humeri from OIP-1 mice showed a significant increase in bone mineral density and bone mineral content. μCT analysis showed increased trabecular thickness and bone volume. OIP-1 mice have dense sclerotic cortical bone with absence of spongiosa and inadequate formation of marrow spaces compared to wild-type mice. Moreover, complete inhibition of osteoclasts and marrow cavities in calvaria suggests defective bone resorption in these mice. OIP-1 mouse bone marrow cultures demonstrated a significant decrease (41%) in osteoclast progenitors and inhibition (39%) of osteoclast differentiation/bone resorption. Western blot analysis further demonstrated suppression of TRAF-2, c-Fos, p-c-Jun, and NFATc1 levels in RANKL-stimulated osteoclast precursors derived from OIP-1 mice. Therefore, OIP-1 is an important physiological inhibitor of osteoclastogenesis and may have therapeutic value against bone loss *in vivo*.

Keywords: osteoclast inhibitory peptide-1/human Sca; osteoclast; osteopetrosis; bone resorption; osteoblast

Introduction

The osteoclast (OCL) is the bone resorbing cell derived from the monocyte/macrophage lineage. OCL formation and bone resorption are regulated by local factors present in the bone marrow micro-environment. Tumour necrosis factor (TNF) gene family member, receptor activator of nuclear factor κB (RANK), expressed on OCL precursors, and RANK ligand (RANKL), expressed on osteoblast/stromal cells, interaction is critical for OCL differentiation and bone resorption [1]. RANK–RANKL signalling promotes the binding of TNF receptor associated factor (TRAF) family proteins such as TRAF-6 to RANK, which results in the activation of Jun N-terminal kinase (JNK) pathways [2]. We have previously identified and characterized a novel autocrine/paracrine inhibitor of OCL formation termed osteoclast inhibitory peptide-1 (OIP-1/hSca) [3]. OIP-1/hSca is a *Ly-6* gene family member expressed on immature thymocytes and thymic epithelial cells [4]. OIP-1/hSca is a glycophosphatidylinositol (GPI)-linked membrane protein (16 kD) containing a 79-amino acid extracellular peptide and a 32-amino acid carboxy-terminal GPI-linked peptide (c-peptide). OIP-1/hSca is a human homologue of mouse *Sca-2* with 65% identity at the nucleotide level, with a conserved pattern of cysteine residues in protein structure [5]. Previously, we have demonstrated that the OIP-1 c-peptide region is critical for OCL inhibitory activity and that a neutralizing antibody against the c-peptide completely blocks OIP-1 activity to inhibit OCL formation *in vitro*; however, a role in skeletal development is unknown [6]. We have also shown that OIP-1/hSca mRNA is highly expressed in osteoblastic cells, OCLs, and bone marrow cells, and that the hSca protein is cleavable from the OCL surface [3]. It has been demonstrated that Sca-2 functions as a modulator of the T-cell receptor (TCR) signalling pathway [7]. In addition, it has been shown to be physically and functionally associated with CD3 ζ chains of the TCR complex [8]. Furthermore, *Ly*-6A knock-out mice demonstrated a significant decrease in bone mineral density and bone mineral content compared with wild-type mice [9].

These studies implicate an essential role for the *Ly-6* gene family in normal bone remodelling. In this study, we show that transgenic mice with OIP-1/hSca over-expression targeted to the osteoclast lineage develop an osteopetrotic bone phenotype through inhibition of OCL formation/activity *in vivo*.

Materials and methods

Development of OIP-1 transgenic mice

Human OIP-1 cDNA was excised from the CDS 5-3 plasmid by BamH1 and PmeI digestion. The resulting DNA fragment (430 bp) encoding the complete coding sequence of OIP-1 was sub-cloned into the pKCR3ΔR1-mTRAP gene promoter containing plasmid (Figure 1A). The transgene fragment from the plasmid construct (pKCR3ΔR1-mTRAP-OIP-1#4) was micro-injected into the male pronucleus of fertilized one-cell mouse embryos at 3 μg/ml concentration and re-implanted into the oviducts of pseudo-pregnant female mice as previously described [10]. The presence of the transgene was identified in resulting offspring by polymerase chain reaction (PCR) screening with OIP-1 gene-specific primers [6] using template genomic DNA purified from a small piece of tail taken from each animal at the time they were

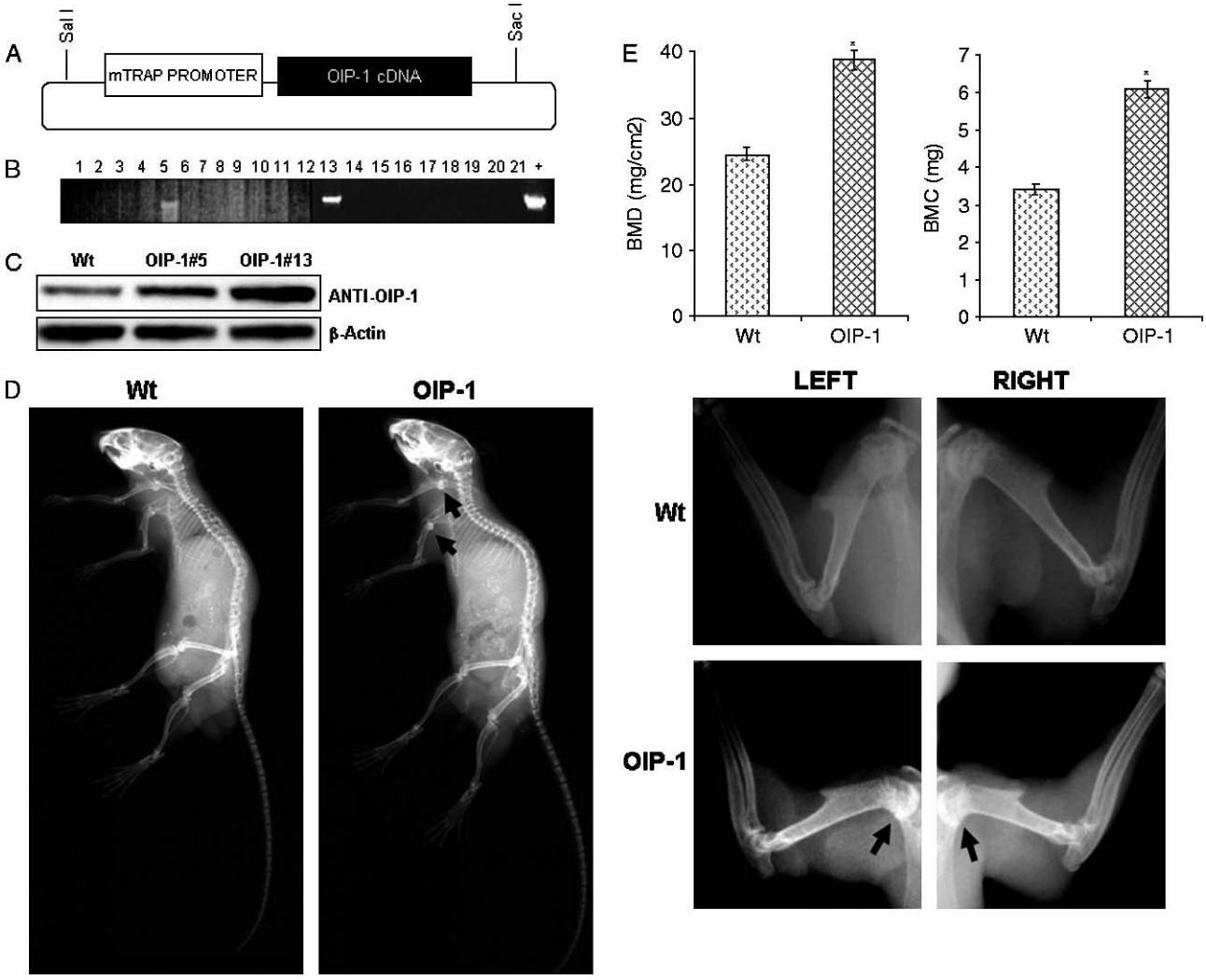

Figure 1. OIP-1 transgenic mice exhibit focal osteopetrotic bone phenotype. (*A*). mTRAP-OIP-1 transgene plasmid map. The mTRAP-OIP-1 transgene fragment (4 Kb) was excised by Sal-I-Sac I digestion from the plasmid PKCR3ΔR1 mTRAP-OIP#4 for micro-injection into the mouse embryos to develop OIP-1 transgenic mice. (*B*). PCR screening of potential founder mice with OIP-1 gene specific primers as described in methods. PCR product amplified using the transgene plasmid served as a positive control (+). We thus identified two potential founder mouse lines #5 and#13. (C) Western blot analysis of OIP-1 expression in transgenic mouse derived preosteoclast cells. Non-adherent bone marrow cells obtained from wild-type (Wt) and OIP-1 transgenic mice were cultured at a density of 1×10^6 cells for 4 days in the presence of 10 ng/ml M-CSF and 100 ng/ml RANKL to obtain preosteoclast cells. Total cell lysates obtained were subjected to Western blot analysis using rabbit anti-OIP-1 antibody. (D) Radiological analysis of the wild-type (Wt) and OIP-1 transgenic mice were performed using a Faxitron MX20 equipped with a FPX-2 Imaging system. Magnified radiographs of left and right humerus of Wt and OIP-1 mice (4 week old) showed increased radiodensity in the proximal humeral region as pointed by arrows. (E) Bone mineral density (BMD) and Bone mineral content (BMC) of Wt and OIP-1 mice humerus bones at 4 weeks of age as measured by dual energy X-ray absorptiometry (DEXA) and values represent mean ± SD ($n = 5$; $p < 0.05$)

weaned. We thus identified two potential founder lines (Nos 5 and 13) of OIP-1 transgenic mice (Figure 1B). Western blot analysis further confirmed high levels of OIP-1 expression in pre-osteoclast cells derived from these founder lines compared with wild-type mice (Figure 1C). All experiments were performed using OIP-1 mice, line 13 (3 to 4 weeks old), unless otherwise specified, with appropriate littermate controls, following the Institutional Animal Care and Use Committee (IACUC) procedure approved by the Institutional Review Board.

Micro-computed tomography (μCT) analysis

The bones collected from 4-week-old mice were fixed in 70% ethanol and the distal metaphyses were scanned with a Skyscan 1072 μCT instrument and analysed by CT-Analyzer software (SkyScan). Two-dimensional images were used to generate three-dimensional reconstructions and to calculate morphometric parameters.

Histology and histomorphometric analysis

The wild-type and OIP-1 mouse bone specimens were fixed in 4% paraformaldehyde in phosphate-buffered saline (PBS), decalcified in 0.5 M EDTA (pH 7.4) for a 1 to 3-week period, and processed for paraffin embedding. Serial 5-μm sections were cut on a modified Leica RM 2155 rotary microtome (Leica Microsystems, Ontario, Canada) and stained with haematoxylin and eosin [11].

In order to perform histochemical staining, bone specimens were fixed overnight in 70% ethanol and embedded in methyl methacrylate (MMA). Serial 4 to 6-μm sections of MMA embedded calvaria were sectioned from anterior to posterior through frontal and parietal bone tissues and humerus sections were stained for tartrate resistant acid phosphatase (TRAP) activity using a histochemical kit (Sigma). Alkaline phosphatase activity and Goldner trichrome staining were performed as previously described [12,13]. Histomorphometric analysis was performed with OsteoMeasure version 2.2 software.

Osteoclast culture and bone resorption activity assays

Wild-type and OIP-1 transgenic mouse bone marrow cells were cultured to form OCLs as previously described [6]. Bone marrow-derived non-adherent cells (1.3×10^6 per ml) were cultured in 24-well plates in the presence of mRANKL (5–100 ng/ml) and M-CSF (10 ng/ml) for 5 days. At the end of the culture period, the cells were fixed with 2% glutaraldehyde in PBS for 20 min and stained for TRAP activity. TRAP-positive multinucleated OCLs containing three or more nuclei were scored microscopically.

To determine the bone resorption activity, wild-type and OIP-1 transgenic mouse bone marrow cells treated with 10 ng/ml mM-CSF for 12 h, and non-adherent bone marrow mononuclear cells (1×10^6 cells per well) were cultured to form OCLs on sterile dentine slices for 10 days as previously described [6]. The cells were removed using 1 M NaOH and stained with 0.1% toluidine blue. The areas of resorption lacunae on the digital images were quantified. The percentage of resorbed area was calculated relative to the total dentine disc area.

Western blot analysis for RANK receptor signalling molecules in OIP-1 transgenic mouse-derived pre-osteoclasts and immunocytochemical staining of OIP-1 expression in osteoclast cells were performed using rat anti-mouse TSA-1/Sca MAb (PharMingen, CA, USA) [14].

Osteoblast differentiation

Wild-type and OIP-1 transgenic mouse bone marrow-derived stromal/pre-osteoblast cells were cultured with medium containing 10 mM glycerophosphate and 50 μg/ml ascorbic acid for an indicated period (0–12 days). The total RNA (2 μg) isolated was reverse-transcribed using random hexamers and Moloney murine leukaemia virus reverse transcriptase (Applied Biosystems, CA, USA). The resulting cDNAs were then amplified by PCR using osteoblast marker gene-specific primers for osteocalcin, alkaline phosphatase, collagen type I, and β-actin control primers as previously described [15].

Statistical analysis

Data are presented as mean and the statistical analysis between the wild-type and OIP-1 transgenic mice for a given parameter was established by Student's t-test, with $p < 0.05$ considered statistically significant. Statistical analysis of skeletal parameters was also applied by one-way ANOVA.

Results

OIP-1 mice show osteopetrotic bone phenotype

We have previously identified and characterized the osteoclast inhibitory peptide-1 (OIP-1/hSca), which inhibits osteoclast formation and bone resorption activity *in vitro*; however, a role for OIP-1 in skeletal development is unknown [6]. To define a functional role for OIP-1 in bone remodelling, we developed transgenic mice in which OIP-1 expression is targeted to the osteoclast lineage using the mouse TRAP gene promoter as described in the Materials and methods section. OIP-1 transgenic mice that are heterozygous were born normal and fertile; however, there was no significant difference in overall body size compared with non-transgenic littermates. OIP-1 mice showed normal tooth eruption and no visible deformity, or in the growth of the skeleton, compared with wild-type mice. Interestingly, the radiographic analysis of OIP-1 transgenic mice showed an increased

radiodensity of the proximal humerus when compared with wild-type mice of 4-week-old littermates, indicating an osteopetrotic bone phenotype in OIP-1 mice (Figure 1D). To confirm the increased radio-opacity in the humerus of OIP-1 mice, bone mineral density (BMD) and bone mineral content (BMC) were measured by DEXA. The humeral region of 4-week-old OIP-1 mice showed a significant increase in BMD (58.36%) and in BMC (79.41%) (Figure 1E). μCT analysis also demonstrated a significant increase in trabecular thickness, bone volume, and bone surface in the humeral region of OIP-1 mice (Figures 2A–2D) compared with wild-type littermates. Furthermore, μCT analysis of the vertebral region of OIP-1 mice showed an increased trabecular thickness, trabecular bone volume, and bone surface compared with wild-type mice (Figures 2E–2H).

To analyse the osteopetrotic bone phenotype further, we examined the humeri from the OIP-1 mice histologically. The altered growth zone at the proximal end in the humerus of 4-week-old OIP-1 transgenic mice is shown in Figure 3A. OIP-1 mice exhibited absence of primary and secondary spongiosa and inadequate formation of marrow spaces. Much of the epiphysis consisted of dense sclerotic cortical bone, suggesting defective bone resorption in OIP-1 mice. The solid block of bone below the growth plate obliterating the marrow cavity varied in severity in the majority (>85%) of OIP-1 mice at 3 to 4 weeks old. The growth plate region appeared distorted due to the decreased marrow space rather than a significant change in the height or premature closure. To clarify further that the osteopetrotic bone phenotype in OIP-1 mice was due to OIP-1 inhibition of OCL development, we evaluated the OCL numbers in histological specimens by staining for TRAP activity (Figure 3B). Histomorphometric analysis identified a significant decrease (46.16%) in the number of TRAP-positive OCLs in the humeri from OIP-1 mice compared with wild-type littermates (Figure 3C). However, the number of osteoblast cells per bone perimeter area was not affected in humeri from OIP-1 mice compared with wild-type mice (Figure 3D). In addition, calvaria from the OIP-1 mice demonstrated inhibition of TRAP-positive OCLs at the endosteal bone surfaces and underdeveloped bone marrow spaces compared with wild-type littermates (Figure 4A). Furthermore, as evident from the alkaline phosphatase activity staining, there was no significant change in osteoblastic activity on periosteal and endosteal bone surfaces (Figure 4B). Also, calvarial sections showed normal osteoid seams

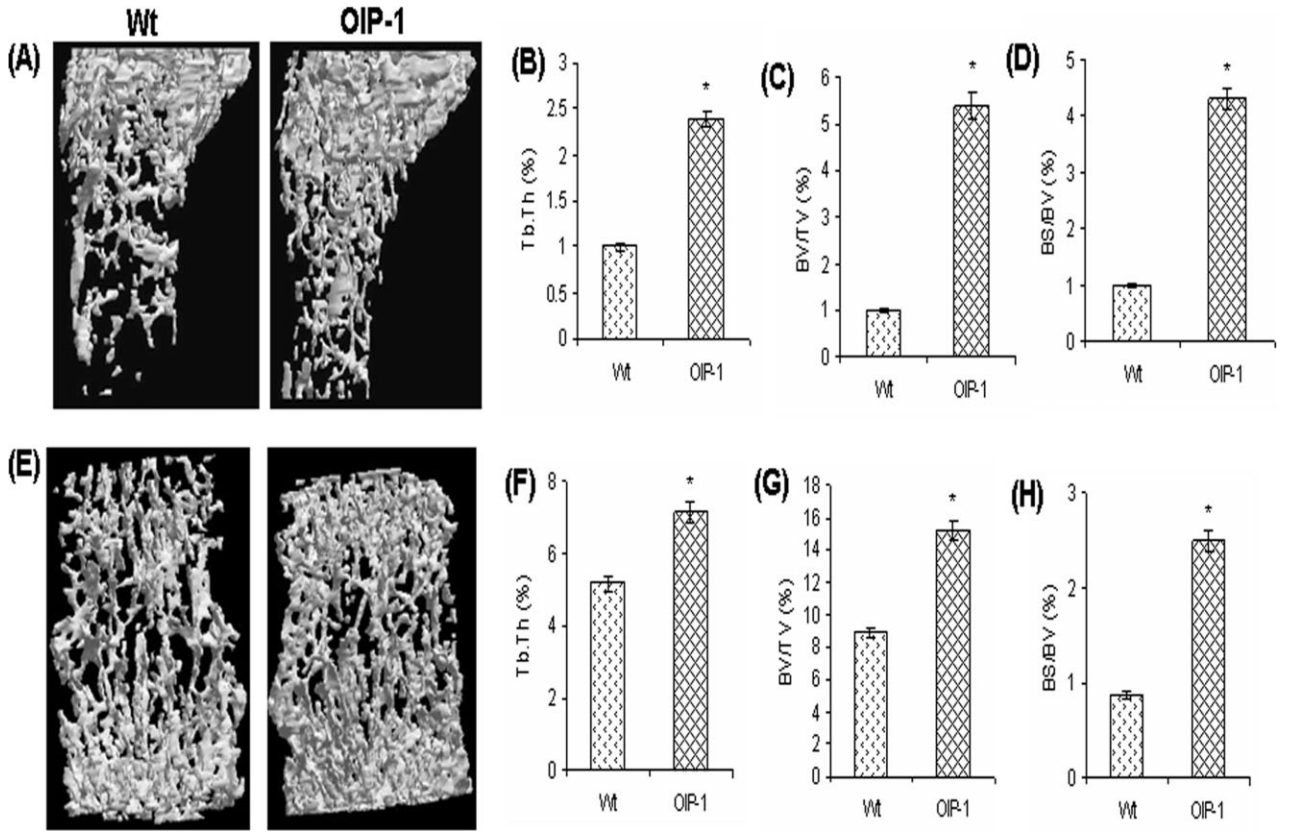

Figure 2. μCT analysis of bones from 4 week old wild-type (Wt) and OIP-1 mice. (A) μCT images showed increased bone mass in the humeral region of OIP-1 mice compared to wild-type littermates. (B) Quantification of trabecular thickness (TbTh). (C) trabecular bone volume (bone volume per tissue volume, BV/TV) and (D) bone surface/volume (BS/BV) in the humeral region of wild-type and OIP-1 mice. (E) μCT images of the lumber vertebrae from OIP-1 mice compared to wild-type littermates. (F) Quantification of trabecular thickness (TbTh). (G) trabecular bone volume (BV/TV) and (H) bone surface/volume (BS/BV) in the vertebral region of wild-type and OIP-1 mice. Values represent mean ± SD ($n = 5$; $p < 0.05$)

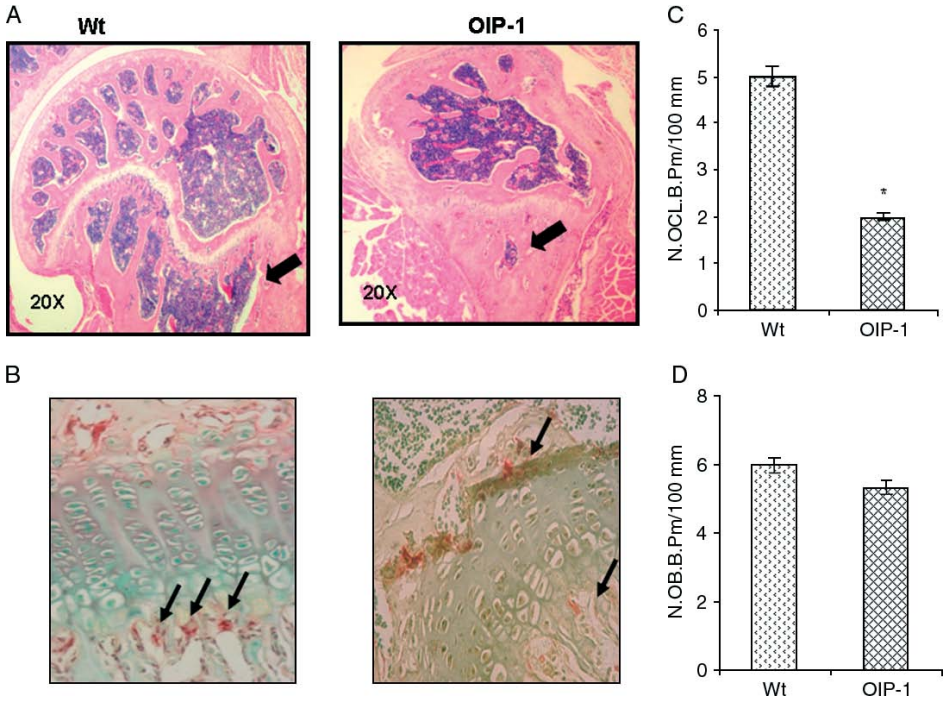

Figure 3. Histological and immunohistochemical analysis of humeri from wild-type (Wt) and OIP-1 mice. (A) Haematoxylin and eosin staining of the growth zone of the proximal end of the humerus of OIP-1 and Wt mice. OIP-1 mice show the osteopetrotic-like bone phenotype with inadequate formation of marrow spaces (as shown by an arrow). Original magnification: ×20. (B) Histochemical staining for TRAP-positive OCLs present at the growth plate region of humeri from Wt and OIP-1 mice (4 weeks old). The TRAP(+) OCLs are indicated by arrows. Original magnification: ×200. (C) Histomorphometric analysis of the number of osteoclasts/bone perimeter (N.OCL/B.Pm/100 mm) and (D) the number of osteoblast/bone perimeter (N.OB/B.Pm/100 mm) in humeri of Wt and OIP-1 mice; values represent mean ± SD ($n = 5$; $p < 0.05$)

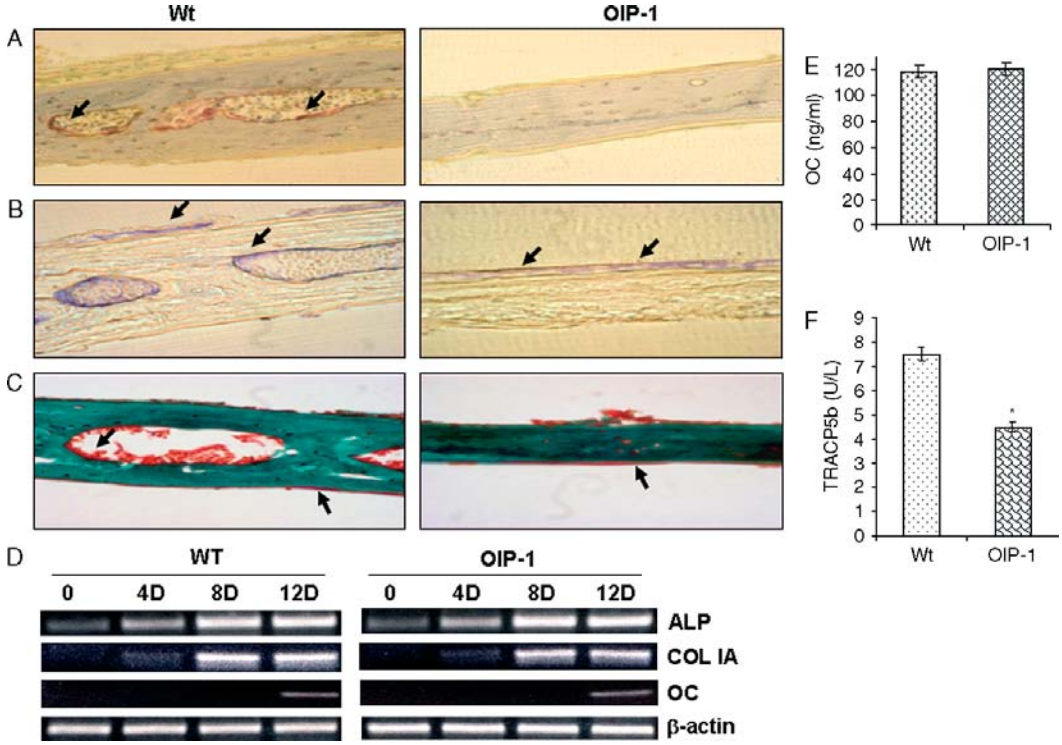

Figure 4. Histological analysis of wild-type (Wt) and OIP-1 transgenic mouse calvaria. (A) Wt mice show TRAP(+) OCLs on the endosteal bone surface of marrow cavities, as indicated by arrows. OIP-1 mouse calvaria showed absence of TRAP(+) OCLs and underdeveloped bone marrow spaces ($n = 10$). (B) Calvaria stained for alkaline phosphatase activity. (C) Goldner's trichrome staining shows osteoid seams on periosteal and endosteal bone surfaces. Original magnification: ×20. (D) Semi-quantitative RT-PCR analysis of osteoblast marker genes, alkaline phosphatase (ALP), collagen type IA (COL IA), and osteocalcin (OC) expression levels in Wt and OIP-1 mouse bone marrow-derived osteoblast cultures. Total RNA isolated from the Wt and OIP-1 mouse bone marrow-derived stromal/pre-osteoblast cells cultured with osteogenic medium for the period indicated (0–12 days) was subjected to RT-PCR analysis for osteoblast differentiation markers as described in the Materials and methods section. ELISA analysis of serum (E) osteocalcin and (F) TRACP5b levels in OIP-1 and Wt mice as noted in the Materials and methods section

on the periosteal and endosteal bone surfaces of both OIP-1 and wild-type mice (Figure 4C).

RT-PCR analysis of the total RNA isolated from osteoblast cells derived from the OIP-1 mouse bone marrow cultures did not show a significant difference in the expression levels of osteoblast differentiation marker genes such as alkaline phosphatase, type I collagen, and osteocalcin gene expression compared with wild-type littermates (Figure 4D). Furthermore, ELISA analysis demonstrated no significant change in the serum osteocalcin levels in OIP-1 mice (Figure 4E). However, the osteoclast activity marker, serum TRAcP5b, was significantly reduced in the OIP-1 transgenic mice, compared with wild-type littermates (Figure 4F). Collectively, these results indicate an osteopetrotic bone phenotype in OIP-1 mice due to inhibition of OCL formation/activity *in vivo*, and that OIP-1 does not modulate bone formation.

Inhibition of osteoclastogenesis in OIP-1 mouse bone marrow cultures

We next performed *ex vivo* experiments using bone marrow cells isolated from the OIP-1 and control mice to assess OIP-1 inhibition of OCL formation. Non-adherent bone marrow cells derived from the wild-type and OIP-1 mice were cultured in the presence of hGM-CSF (10 ng/ml) in methyl cellulose (1.2%) to form CFU-GM colonies. As shown in Figure 5A, OIP-1 transgenic mouse line 5 and 13-derived cells showed a significant decrease in the number of CFU-GM colonies, by 35% and 41% respectively, compared with control mice. We further examined the capacity for OCL differentiation and bone resorption by OIP-1 transgenic mouse-derived bone marrow cells. OIP-1 mouse and wild-type mouse derived non-adherent bone marrow cells were stimulated with various concentrations of RANKL (5–100 ng/ml) with M-CSF (10 ng/ml), and the number of TRAP-positive multinucleated OCLs formed in these cultures was scored. As shown in Figure 5B, the number of OCLs formed in OIP-1 No 5 and OIP-1 No 13 mouse bone marrow cultures was significantly decreased, by 39% and 42% respectively, compared with control mice in response to RANKL (100 ng/ml) treatment. Immunocytochemical staining further confirmed OIP-1 transgene expression in OCLs formed in OIP-1 mouse bone marrow cultures (Figure 5C). As is evident from the osteopetrotic bone phenotype in OIP-1 mice, it is likely that OIP-1 inhibits the bone resorption capacity of OCLs in these mice. We therefore further examined the bone resorption capacity of OCLs formed in OIP-1 mouse bone marrow cultures. As shown in Figures 5D and 5E, OCLs formed in OIP-1 No 5 and OIP-1 No 13 mouse bone marrow cultures demonstrated a significant decrease (39%) in resorption area on dentine slices compared with wild-type mice when cultured in the presence of M-CSF (10 ng/ml) and RANKL (100 ng/ml). These data indicate that targeted overexpression of OIP-1 to the OCL lineage results in significant inhibition of osteoclastogenesis and bone resorption activity *in vivo*.

RANK receptor signalling in pre-osteoclast cells from OIP-1 mice

RANKL–RANK signalling plays a critical role in OCL differentiation and bone resorption activity. We have also demonstrated that OIP-1 c-peptide treatment of RAW 264.7 mouse macrophage cells inhibits OCL formation through the suppression of molecules associated with RANKL–RANK signalling during OCL differentiation [14]. We therefore further examined the status of RANK receptor signalling molecules such as TRAF-2, ERK, JNK, c-Fos, and NFATc1 which are responsive to RANKL stimulation of OIP-1 mouse bone marrow cultures [16]. Non-adherent bone marrow cells derived from the wild-type and OIP-1 transgenic mice were stimulated with M-CSF (10 ng/ml) and RANKL (100 ng/ml) for 48 h. Western blot analysis of total cell lysates obtained from these pre-osteoclast cells identified no significant changes in the levels of RANK receptor expression. In contrast, RANK adaptor protein TRAF-2 expression, but not TRAF-6, was significantly decreased (ten-fold) in OIP-1 transgenic mouse-derived cells compared with wild-type mice. OIP-1 mouse-derived pre-osteoclasts also demonstrated a three-fold decrease in the levels of c-Fos and NFATc1 (Figure 6A).

We further examined the activation status of extracellular signal-regulated kinases (ERK) and c-Jun N-terminal kinase (JNK) molecules in response to RANKL stimulation of OIP-1 mouse bone marrow cells. As shown in Figure 6B, OIP-1 mouse-derived pre-osteoclast cells showed a time-dependent inhibition of ERK phosphorylation in response to RANKL stimulation, compared with wild-type mice. Similarly, JNK activation was significantly decreased in OIP-1 mouse pre-osteoclast cells compared with wild-type mice (Figure 6C). Taken together, OIP-1 inhibits OCL formation and bone resorption activity through the suppression of RANK receptor signalling molecules. These results further support the osteopetrotic bone phenotype in OIP-1 transgenic mice.

Discussion

We have previously reported on OIP-1/hSca as an autocrine/paracrine inhibitor of OCL formation and bone resorption activity [3,6]. Expression of OIP-1 mRNA in early and more committed OCL cell lineages and osteoblasts [17] suggested that OIP-1/hSca may play an important role in OCL formation. Immune cell products such as interferon (IFN)-γ are potent inhibitors of OCL formation. We have previously shown that IFN-γ stimulates OIP-1/hSca expression in OCL precursor cells [14]. It is more likely, therefore, that OIP-1 is an important physiological regulator of osteoclast development and bone resorption activity *in vivo*. Previously it has been shown

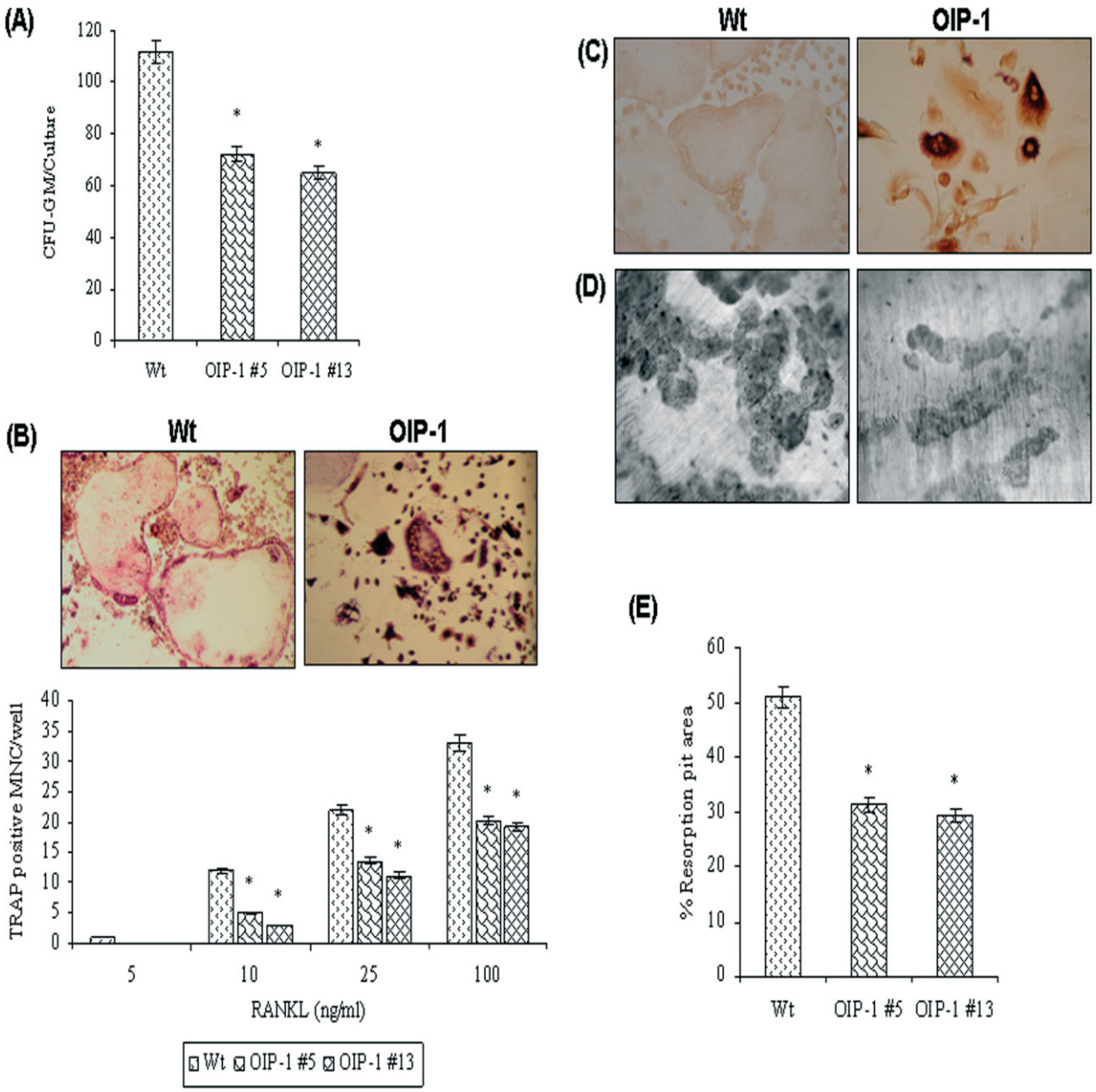

Figure 5. Inhibition of osteoclastogenesis in OIP-1 mouse bone marrow cultures. (A) CFU-GM formation in OIP-1 mouse bone marrow cultures. Wild-type (Wt) and OIP-1 mouse derived non-adherent bone marrow cells (4×10^5/ml) were cultured with hGM-CSF (10 ng/ml) in 1.2% methyl cellulose to form CFU-GM colonies. At the end of a 7 day culture period, CFU-GM colonies (aggregates $>$50 cells) formed in these cultures were scored using a light microscope as described earlier [7]. (B) Wild-type (Wt) and OIP-1 transgenic mouse bone marrow derived non-adherent cells were stimulated with RANKL (5–100 ng/ml) and M-CSF (10 ng/ml) for 5 days and the TRAP (+) multinucleated OCLs formed in these cultures were scored. The results represent quadruplicate cultures of three independent experiments ($p < 0.05$). (C) Immune staining for OIP-1/hSca expression in OCL formed in Wt and OIP-1 mouse bone marrow cultures was performed using rat anti-mouse TSA-1/Sca-2 antibody at a concentration of 1 μg/ml. Photomicrographs were taken at magnification ×20. (D) Wt and OIP-1 mouse bone marrow derived non-adherent cells (1×10^6) were cultured to form OCL as described on dentine slices for 10 days. The cells were removed by treating the disc with 1 M NaOH and stained with 0.1% toluidine blue. Resorption lacunae formed on dentine slices were identified by light microscopy. (E) The percentage of resorbed area on dentine was quantified as described in the methods. The results represent quadruplicate cultures of three independent experiments ($p < 0.05$)

that c-Src, a proto-oncogene deficiency, causes severe osteopetrosis in mice which lacks tooth eruption. The OCL development is normal in Src-deficient mice; however, the OCLs cannot form ruffled borders to resorb bone [18]. In contrast, OIP-1 mice show normal tooth eruption and no significant difference in body size. However, μCT analysis indicated an osteopetrosis bone phenotype in OIP-1 mice. Also, DEXA analysis showed a significant increase in BMD and BMC in the humeri from OIP-1 mice. Recently it has been reported that mice lacking the immunomodulatory adapter proteins DAP12 and Fc receptor gamma chain (FcRγ) exhibit severe osteopetrosis; however, they develop teeth, distinguishing their phenotype from $Src^{-/-}$ and RANKL-deficient mice [19].

Histological analysis indicated inadequate formation of marrow spaces in calvaria and humeri of OIP-1 mice. Histomorphometric analysis of humeri and

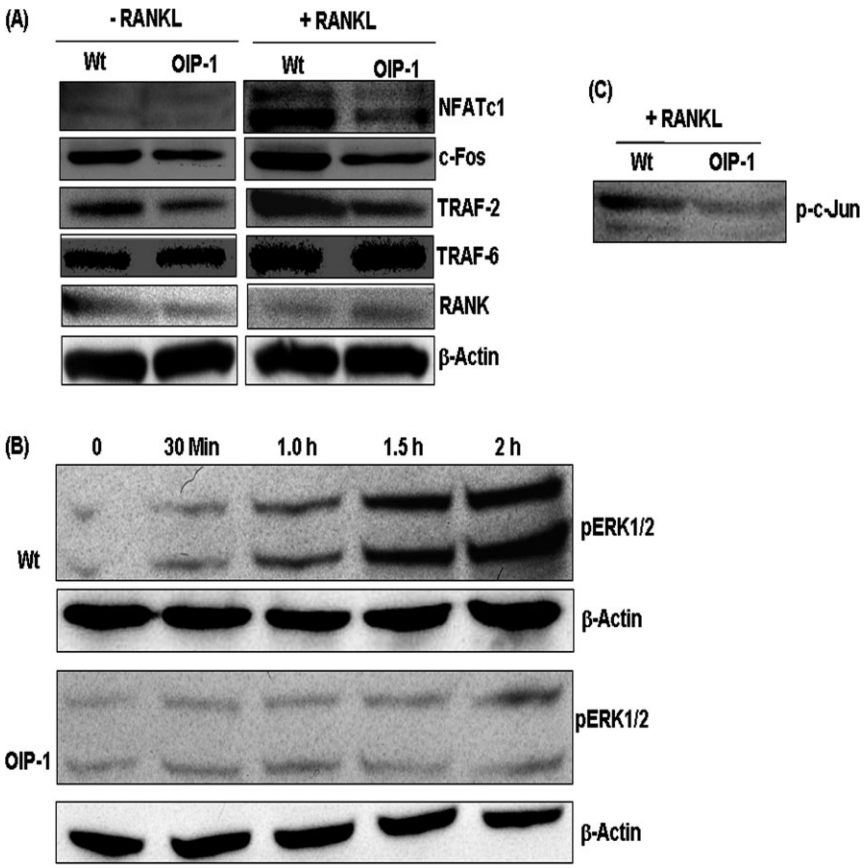

Figure 6. Western blot analysis of RANK receptor associated signaling molecules during OCL differentiation. (A) Wild-type (Wt) and OIP-1 mouse derived bone marrow cells were cultured in the presence of 10 ng/ml M-CSF for 24 h. The non-adherent cells were treated with M-CSF (10 ng/ml) and stimulated with or without RANKL (100 ng/ml) for 2 days. Total cell lysates prepared from the preosteoclast cells were subjected to Western blot analysis for TRAF2, TRAF6, c-Fos and NFATc1. β-actin expression levels were also analyzed to normalize the protein loading onto the gels in all the samples. (B) The preosteoclast cells were incubated with RANKL (100 ng/ml) for an indicated period and expression of pERK was determined. (C) JNK activity in the preosteoclast cells derived from Wt and OIP-1 mice

calvaria further demonstrated a significant decrease in OCL development. In contrast, femurs from OIP-1 mice had no significant change in the numbers of TRAP-positive osteoclasts; however, they demonstrated a significant change in bone volume (data not shown). These results indicate OIP-1-specific inhibition of osteoclast formation/activity *in vivo*. Furthermore, our results that the number of osteoblasts per bone perimeter area was not affected in OIP-1 mice compared with control mice and that there was a lack of significant differences in the levels of serum osteocalcin and osteoblast-specific gene expression in OIP-1 mice compared with wild-type mice suggest that bone formation is not affected in these mice.

Mouse bone marrow culture studies *ex vivo* further suggested that the osteopetrotic bone phenotype is due to a significant decrease in OCL number and activity compared with control mice. These results are consistent using bone marrow cells derived from two of the founder lines established with comparable levels of OIP-1 expression. It is possible that genomic integration of the OIP-1 transgene may influence the severity of the osteopetrotic bone phenotype in these mice. We have further confirmed OIP-1-specific inhibition of OCL differentiation of RAW cells *in vitro* through constitutive overexpression (data not shown). Our results are therefore consistent with an osteopetrotic phenotype due to inhibition of osteoclastogenesis and bone resorption activity in OIP-1 mice.

Earlier we demonstrated that OIP-1 significantly decreased RANKL-induced JNK activity in RAW 264.7 cells. Furthermore, OIP-1 decreased TRAF-2 expression in pre-osteoclast cells, but had no significant effect on TRAF-6 and RANK expression in these cells [14]. These data suggest that targeted overexpression of OIP-1 to the OCL lineage *in vivo* results in inhibition of OCL differentiation through suppression of TRAF-2 and JNK activity. Although TRAF-2 is essential for TNF-α-induced osteoclastogenesis and TRAF-5 functions in both RANKL and TNF-α-induced osteoclastogenesis [20,21], our results indicate that OIP-1 suppresses RANK receptor signalling through TRAF-2, but not TRAF-6, to inhibit OCL differentiation. It is possible that TRAF-2 interaction with other signalling molecules may play an important role in downstream signalling that is necessary to activate JNK activity during OCL differentiation. ERK has been implicated in cellular proliferation, migration, and survival [22]. Thus, inhibition of ERK activation in OIP-1 mouse-derived pre-osteoclast

cells further supports our results indicating a significant decrease in the growth of early OCL precursors, CFU-GM. NFATc1 is a critical transcription factor that modulates OCL-specific genes such as the calcitonin receptor and TRAP expression during OCL differentiation [23–25]. OIP-1 mouse-derived pre-osteoclast cells demonstrated a significant decrease in the level of NFATc1 expression in response to RANKL stimulation compared with wild-type mice. It is therefore possible that NFATc1 may play a critical role in OIP-1 function as a downstream effector to suppress gene expression during OCL differentiation.

In summary, OIP-1/hSca represents a novel physiological inhibitor of osteoclast development and bone resorption *in vivo*. Thus, OIP-1 may have therapeutic utility for bone disease with high bone turnover, such as osteoporosis and Paget's disease of bone.

Acknowledgements

This work was supported by the National Institute of Health grant DE 12603, a DOD Medical Research Award, and grant C06RR015455 from the Extramural Research Facilities Program of the National Center for Research Resources.

References

1. Suda T, Takahashi N, Udagawa N, Jimi E, Gillespie MT, Martin TJ. Modulation of osteoclast differentiation and function by the new members of the tumor necrosis factor receptor and ligand families. *Endocr Rev* 1999;**20:**345–357.
2. Hsu H, Lacey DL, Dunstan CR, Solovyev I, Colombero A, Timms E, *et al*. Tumor necrosis factor receptor family member RANK mediates osteoclast differentiation and activation induced by osteoprotegerin ligand. *Proc Natl Acad Sci U S A* 1999;**96:**3540–3545.
3. Choi SJ, Devlin RD, Menaa C, Chung H, Roodman GD, Reddy SV. Cloning and identification of human Sca as a novel inhibitor of osteoclast formation and bone resorption. *J Clin Invest* 1998;**102:**1360–1368.
4. Palfree RG. Ly-6-domain proteins — new insights and new members: a C-terminal Ly-6 domain in sperm acrosomal protein SP-10. *Tissue Antigens* 1996;**48:**71–79.
5. Capone MC, Gorman DM, Ching EP, Zlotnik A. Identification through bioinformatics of cDNAs encoding human thymic shared Ag-1/stem cell Ag-2. A new member of the human Ly-6 family. *J. Immunol* 1996;**157:**969–973.
6. Koide M, Kurihara N, Maeda H, Reddy SV. Identification of the functional domain of osteoclast inhibitory peptide-1/hSca. *J Bone Miner Res* 2002;**17:**111–118.
7. Kosugi A, Saitoh S, Narumiya S, Miyake K, Hamaoka T. Activation-induced expression of thymic shared antigen-1 on T lymphocytes and its inhibitory role for TCR-mediated IL-2 production. *Int Immunol* 1994;**6:**1967–1976.
8. Kosugi A, Saitoh S, Noda S, Miyake K, Yamashita Y, Kimoto M, *et al*. Physical and functional association between thymic shared antigen-1/stem cell antigen-2 and the T cell receptor complex. *J Biol Chem* 1998;**273:**12301–12306.
9. Bonyadi M, Waldman SD, Liu D, Aubin JE, Grynpas MD, Stanford WL. Mesenchymal progenitor self-renewal deficiency leads to age-dependent osteoporosis in Sca-1/Ly-6A null mice. *Proc Natl Acad Sci U S A* 2003;**100:**5840–5845.
10. Hogan BBR, Costantini F, Lacy E. *Manipulating the Mouse Embryo*. Cold Spring Harbor Laboratory Press: Plainview, NY, 1994.
11. Richard S, Torabi N, Franco GV, Tremblay GA, Chen T, Vogel G. Ablation of the Sam68 RNA binding protein protects mice from age-related bone loss. *PLoS Genet* 2005;**1:**e74.
12. Horn DA, Garrett IR. A novel method for embedding neonatal murine calvaria in methyl methacrylate suitable for visualizing mineralization, cellular and structural detail. *Biotech Histochem* 2004;**79:**151–158.
13. Parfitt AM, Drezner MK, Glorieux FH, Kanis JA, Malluche H, Meunier PJ. Bone histomorphometry: standardization of nomenclature, symbols, and units. Report of the ASBMR Histomorphometry Nomenclature Committee. *J Bone Miner Res* 1987;**2:**595–610.
14. Koide M, Maeda H, Roccisana JL, Kawanabe N, Reddy SV. Cytokine regulation and the signaling mechanism of osteoclast inhibitory peptide-1 (OIP-1/hSca) to inhibit osteoclast formation. *J Bone Miner Res* 2003;**18:**458–465.
15. Zhou S, Yates KE, Eid K, Glowacki J. Demineralized bone promotes chondrocyte or osteoblast differentiation of human marrow stromal cells cultured in collagen sponges. *Cell Tissue Bank* 2005;**6:**33–44.
16. Wada T, Nakashima T, Hiroshi N, Penninger JM. RANKL–RANK signaling in osteoclastogenesis and bone disease. *Trends Mol Med* 2006;**12:**17–25.
17. Horowitz MC, Fields A, DeMeo D, Qian HY, Bothwell AL, Trepman E. Expression and regulation of Ly-6 differentiation antigens by murine osteoblasts. *Endocrinology* 1994;**135:**1032–1043.
18. Xing L, Venegas AM, Chen A, Garrett-Beal L, Boyce BF, Varmus HE. Genetic evidence for a role for Src family kinases in TNF family receptor signaling and cell survival. *Genes Dev* 2001;**15:**241–253.
19. Mocsai A, Humphrey MB, Van Ziffle JA, Hu Y, Burghardt A, Spusta SC, *et al*. The immunomodulatory adapter proteins DAP12 and Fc receptor gamma-chain (FcRgamma) regulate development of functional osteoclasts through the Syk tyrosine kinase. *Proc Natl Acad Sci U S A* 2004;**101:**6158–6163.
20. Kanazawa K, Kudo A. TRAF2 is essential for TNF-alpha-induced osteoclastogenesis. *J Bone Miner Res* 2005;**20:**840–847.
21. Kanazawa K, Azuma Y, Nakano H, Kudo A. TRAF5 functions in both RANKL- and TNFalpha-induced osteoclastogenesis. *J Bone Miner Res* 2003;**18:**443–450.
22. Lee SE, Woo KM, Kim SY, Kim HM, Kwack K, Lee ZH. The phosphatidylinositol 3-kinase, p38, and extracellular signal-regulated kinase pathways are involved in osteoclast differentiation. *Bone* 2002;**30:**71–77.
23. Ikeda F, Nishimura R, Matsubara T, Tanaka S, Inoue J, Reddy SV, *et al*. Critical roles of c-Jun signaling in regulation of NFAT family and RANKL-regulated osteoclast differentiation. *J Clin Invest* 2004;**114:**475–484.
24. Crotti TN, Flannery M, Walsh NC, Fleming JD, Goldring SR, McHugh KP. NFATc1 regulation of the human beta3 integrin promoter in osteoclast differentiation. *Gene* 2006;**372:**92–102.
25. Matsuo K, Galson DL, Zhao C, Peng L, Laplace C, Wang KZ. Nuclear factor of activated T-cells (NFAT) rescues osteoclastogenesis in precursors lacking c-Fos. *J Biol Chem* 2004;**279:**26475–26480.

Mutation of the sequestosome 1 (*p62*) gene increases osteoclastogenesis but does not induce Paget disease

Noriyoshi Kurihara,[1,2] Yuko Hiruma,[1,2] Hua Zhou,[3] Mark A. Subler,[4] David W. Dempster,[5] Frederick R. Singer,[6] Sakamuri V. Reddy,[7] Helen E. Gruber,[8] Jolene J. Windle,[4] and G. David Roodman[1,2]

[1]VA Pittsburgh Healthcare System, Research and Development, Pittsburgh, Pennsylvania, USA. [2]Division of Hematology/Oncology, Department of Medicine, University of Pittsburgh, Pittsburgh, Pennsylvania, USA. [3]Regional Bone Center, Helen Hayes Hospital, West Haverstraw, New York, USA. [4]Department of Human Genetics, Virginia Commonwealth University, Richmond, Virginia, USA. [5]Department of Pathology, Columbia University College of Physicians and Surgeons, New York, New York, USA. [6]Endocrine/Bone Disease Program, John Wayne Cancer Institute, Santa Monica, California, USA. [7]Department of Pediatrics, Children's Research Institute, Medical University of South Carolina, Charleston, South Carolina, USA. [8]Department of Orthopaedic Surgery, Carolinas Medical Center, Charlotte, North Carolina, USA.

Paget disease is the most exaggerated example of abnormal bone remodeling, with the primary cellular abnormality in the osteoclast. Mutations in the *p62* (sequestosome 1) gene occur in one-third of patients with familial Paget disease and in a minority of patients with sporadic Paget disease, with the P392L amino acid substitution being the most commonly observed mutation. However, it is unknown how $p62^{P392L}$ mutation contributes to the development of this disease. To determine the effects of $p62^{P392L}$ expression on osteoclasts in vitro and in vivo, we introduced either the $p62^{P392L}$ or WT *p62* gene into normal osteoclast precursors and targeted $p62^{P392L}$ expression to the osteoclast lineage in transgenic mice. $p62^{P392L}$-transduced osteoclast precursors were hyperresponsive to receptor activator of NF-κB ligand (RANKL) and TNF-α and showed increased NF-κB signaling but did not demonstrate increased 1,25-$(OH)_2D_3$ responsivity, TAF_{II}-*17* expression, or nuclear number per osteoclast. Mice expressing $p62^{P392L}$ developed increased osteoclast numbers and progressive bone loss, but osteoblast numbers were not coordinately increased, as is seen in Paget disease. These results indicate that $p62^{P392L}$ expression on osteoclasts is not sufficient to induce the full pagetic phenotype but suggest that *p62* mutations cause a predisposition to the development of Paget disease by increasing the sensitivity of osteoclast precursors to osteoclastogenic cytokines.

Introduction

Paget disease (PD) is the second most common bone disease in persons of Anglo-Saxon descent over the age of 55 (1). It is the most exaggerated example of disordered bone remodeling, with abnormalities in all phases of the bone remodeling process (2). The primary cellular abnormality resides in the osteoclast (OCL). OCLs in PD are increased in number and size and have increased numbers of nuclei (3). In addition, they are hyperresponsive to 1,25-$(OH)_2D_3$ and receptor activator of NF-κB ligand (RANKL) (4, 5) and show increased expression of TAF_{II}-*17*, a member of the $TF_{II}D$ transcription complex, which acts as a coactivator of vitamin D receptor–mediated transcription and is upregulated in pagetic osteoclasts (6).

Both genetic and environmental factors have been proposed as contributing to the etiology of PD, and multiple families with an autosomal dominant mode of inheritance have been described (7, 8). Recently, mutations in the *p62* (sequestosome 1) gene have been linked to approximately 30% of patients with familial PD and to a minority of patients with sporadic PD (8). All of the mutations identified to date lie within or near the ubiquitin-binding domain in the carboxyterminal region of the protein, with the P392L amino acid substitution representing the most frequently observed mutation (8). *p62* plays a critical role in NF-κB activation induced by TNF-α, CD40, and IL-1 through its interactions with the atypical protein kinases ζPKC and λPKC (9, 10). However, the role of *p62* mutations in PD is unclear since not all individuals carrying a *p62* mutation have PD (11–13).

It is our hypothesis that both genetic and nongenetic factors are required for the development of PD and that the genetic factors, such as *p62* mutations, function to increase OCL formation but are not sufficient to induce the abnormal OCLs or pagetic bone lesions characteristic of PD. To test this hypothesis, we characterized OCL precursors from Paget patients carrying the $p62^{P392L}$ mutation as well as control human OCL precursors transduced with either *p62* or $p62^{P392L}$ expression vectors. We also determined whether the $p62^{P392L}$ gene can induce pagetic-like OCLs or bone lesions in vivo when expressed in OCL precursors of transgenic mice.

Results

OCL precursors from PD patients carrying the $p62^{P392L}$ gene are hyperresponsive to RANKL, TNF-α, and 1,25-$(OH)_2D_3$ and express increased levels of TAF_{II}-17. OCL precursors from PD patients carrying the $p62^{P392L}$ mutation or from controls were compared for their capacity to form OCLs over a range of concentrations of RANKL, TNF-α, and 1,25-$(OH)_2D_3$. OCL precursors from patients carry-

Nonstandard abbreviations used: ERK1/2, extracellular signal–regulated kinase 1/2; EV, empty vector; IκB, inhibitor of NF-κB; MVNP, measles virus nucleocapsid protein; OCL, osteoclast; PD, Paget disease; RANKL, receptor activator of NF-κB ligand; TRAP, tartrate-resistant acid phosphatase.

Conflict of interest: The authors have declared that no conflict of interest exists.

Citation for this article: *J. Clin. Invest.* **117**:133–142 (2007). doi:10.1172/JCI28267.

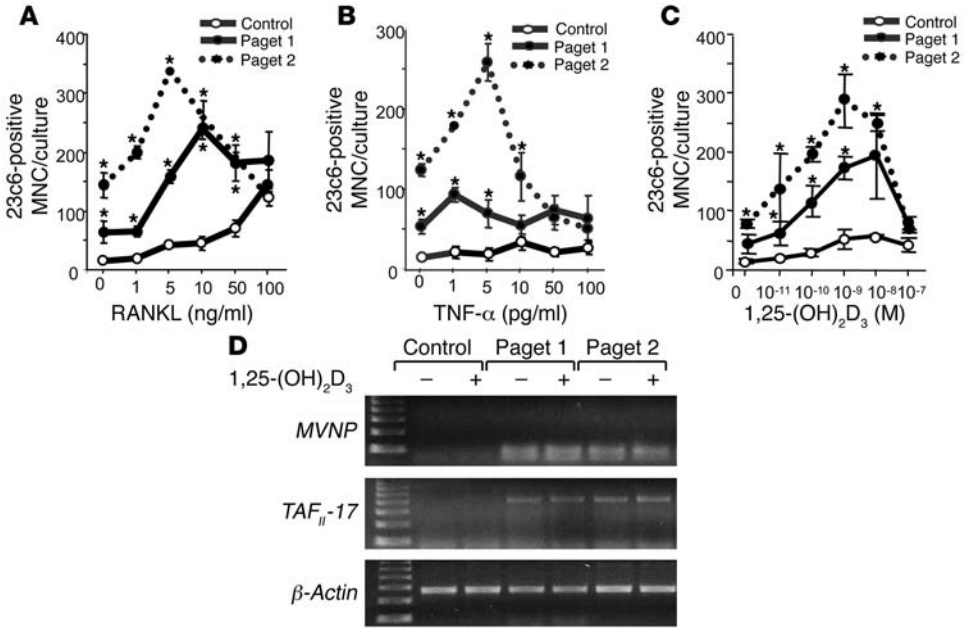

Figure 1
OCL formation and expression of *MVNP* and *TAF$_{II}$-17* in GM-CFU from *p62^{P392L}*-positive PD patients and controls. (**A**–**C**) GM-CFU (10^5 cells/well) from Paget patients known to harbor the *p62^{P392L}* mutation and from normal individuals were cultured for OCL formation in the presence of RANKL (**A**), TNF-α (**B**), or 1,25-$(OH)_2D_3$ (**C**). After 3 weeks of culture, cells were fixed and stained with the 23c6 monoclonal antibody, which identifies OCLs. Results are expressed as the mean ± SEM for quadruplicate determinations. *Significant differences ($P < 0.001$) compared with results from cultures of normal GM-CFU treated with the same concentration of each factor. A similar pattern of results was seen in 2 independent experiments. Paget 1 and Paget 2 refer to PD patient sample groups 1 and 2. MNC, multinuclear cell. (**D**) RT-PCR analysis of *MVNP* and *TAF$_{II}$-17* mRNA expression in GM-CFU from *p62^{P392L}*-positive PD patients and controls cultured for 2 days with 1,25-$(OH)_2D_3$. RT-PCR analysis of β-*actin* expression was included as a control for mRNA quality and amplification.

ing the *p62^{P392L}* mutation were hyperresponsive to RANKL and TNF-α as well as 1,25-$(OH)_2D_3$ (Figure 1, A–C); this is similar to previous findings from patients with sporadic PD (3–5). In cultures of OCL precursors from PD patients with *p62^{P392L}* mutations, maximum OCL formation was obtained at RANKL and TNF-α concentrations of 1–10 ng/ml and 1–10 pg/ml, respectively, compared with 100 ng/ml and 50 pg/ml for normal OCL precursors. Similar results were obtained with 3 individual PD patients. Further, the OCLs that formed contained increased numbers of nuclei per OCL (Table 1) and elevated expression of *TAF$_{II}$-17* (Figure 1D). However, *measles virus nucleocapsid protein* (*MVNP*) transcripts were also present in OCLs from these patients (Figure 1D), raising the possibility that a subset of the phenotypic characteristics of these OCLs might be caused by the presence of *MVNP* rather than *p62^{P392L}*.

OCL formation by p62- and p62^{P392L}-transduced normal OCL precursors. To further dissect the role of *p62^{P392L}* in PD, we transduced normal human OCL precursors with the WT *p62* or *p62^{P392L}* gene or *empty vector* (*EV*). The total p62 expression levels were determined by immunoblotting extracts from transduced GM-CFU–derived cells with an antibody that recognizes both WT and mutant *p62*. The *p62* protein was detected in both *p62*- and *p62^{P392L}*-transduced GM-CFU without treatment with RANKL. In contrast, *p62* protein was only detected in *EV*-transduced GM-CFU after 1 day of treatment with RANKL (data not shown).

p62^{P392L}-transduced OCL precursors treated with varying concentrations of RANKL or TNF-α were found to be hyperresponsive to both cytokines and formed increased numbers of OCLs (Figure 2, A and B). While overexpression of WT *p62* resulted in a degree of hyperresponsivity to RANKL similar to that of *p62^{P392L}*, the *p62^{P392L}* cells were much more hyperresponsive to TNF-α than WT *p62* cells. Both *p62*- and *p62^{P392L}*-transduced OCL precursors formed significantly larger OCLs than EV cells (Figure 2D), although nuclear number per OCL was not increased in *p62*- or *p62^{P392L}*-derived OCLs regardless of treatment (Table 1). Also, a 7-fold increase in bone resorption was observed when OCLs formed by *p62^{P392L}*-transduced human GM-CFU were treated with RANKL (50 ng/ml) and cultured on dentin, as compared with RANKL-treated *EV*-transduced OCLs (Figure 3, A and B).

In contrast with the results with RANKL and TNF-α, neither *p62*- nor *p62^{P392L}*-transduced OCL precursors were hyperresponsive to 1,25-$(OH)_2D_3$ (Figure 2C) or formed increased numbers of OCLs compared with EV-transduced cells. In addition, neither *p62*- nor *p62^{P392L}*-transduced GM-CFU–derived cells showed elevated expression of *TAF$_{II}$-17* in the presence or absence of 10^{-10} M 1,25-$(OH)_2D_3$ (Figure 4).

Effects of p62^{P392L} expression on OCLs in vivo. Since OCLs harbor the primary cellular abnormality in PD, we used the tartrate-resistant acid phosphatase (TRAP) promoter to target expression of the human *p62^{P392L}* gene to the OCL lineage in transgenic mice (TRAP-*p62^{P392L}* mice) to determine the effects of *p62^{P392L}* expression in OCLs in vivo. Eight lines of TRAP-*p62^{P392L}* transgenic mice were generated from independent founder mice, and each of these was characterized with regard to transgene expression level, TNF-α responsivity, and histology. The results described below were obtained from a single line (Tp62m2), although similar results were observed in multiple other lines as well. The expression levels of total *p62* protein in mice of the Tp62m2 line, as determined by immunoblotting of extracts from bone marrow cells with an antibody that detects both murine and human *p62*, were found to be approximately 2.5-fold higher than *p62* levels in WT mice (data not shown).

Histomorphometric evaluation of vertebral bones from TRAP-*p62^{P392L}* mice at 4, 8, 12, and 16 months of age revealed an increase in OCL perimeter (the amount of bone surface covered with TRAP-positive, mono-, and multinuclear cells) and a progressive reduction in cancellous bone volume when compared with that of age-matched WT controls (Table 2 and Supplemental Figure 1; supplemental material available online with this article;

Table 1
Nuclear number per OCL

Cell type	Vehicle	1,25-$(OH)_2D_3$ (10^{-8} M)	RANKL (50 ng/ml)	TNF-α (50 pg/ml)
Control human	10 ± 3	13 ± 2	12 ± 2	13 ± 2
Familial PD	24 ± 3	52 ± 13[A]	32 ± 5[A]	25 ± 4[A]
Human GM-CFU–*EV*	6 ± 3	7 ± 2	12 ± 5	7 ± 2
Human GM-CFU–*p62*^{P392L}	5 ± 3	7 ± 2	10 ± 2	8 ± 2
WT mice	5 ± 3	6 ± 2	9 ± 2	5 ± 2
TRAP-*p62*^{P392L} mice	5 ± 3	6 ± 2	9 ± 2	5 ± 2

The number of nuclei per OCL was determined in 20 random 23c6-positive or TRAP-positive OCLs for each treatment group. Results are expressed as mean ± S.D. [A]Significantly different from the same treatment as the normal donor, $P < 0.01$.

doi:10.1172/JCI28267DS1). The decrease in cancellous bone volume was associated with decreases in both trabecular width and number. Although OCL perimeter was elevated, there was no coupled increase in osteoblast perimeter, as is seen in PD lesions.

Electron microscopic examination of OCLs from TRAP-*p62*^{P392L} mice demonstrated that the cells did not contain the nuclear inclusions characteristic of pagetic OCLs. OCLs were similar to those in WT controls in terms of nuclear and cytoplasmic ultrastructure as well in the morphology of the ruffled border (data not shown).

OCL precursors from TRAP-p62^{P392L} *mice are hyperresponsive to RANKL and TNF-α but not 1,25-$(OH)_2D_3$.* When marrow cells from TRAP-*p62*^{P392L} mice were cultured with RANKL and TNF-α to induce OCL formation, they were found to be hyperresponsive to both cytokines, and they formed increased numbers of OCLs as compared with nontransgenic littermates (Figure 5, A and B). Similarly, treatment of TRAP-*p62*^{P392L} mice with TNF-α (0–1.5 μg/d) significantly increased OCL formation compared with that of WT mice at all concentrations tested (Figure 5, E and G). Further, the dose-response curves for NF-κB reporter gene activity in TRAP-*p62*^{P392L} OCL precursors for both RANKL and TNF-α were shifted to the left compared with cells from WT mice (Figure 5, D and E). However, OCL precursors from TRAP-*p62*^{P392L} mice were not hyperresponsive to 1,25-$(OH)_2D_3$ (Figure 5C) and did not express detectable *TAF_{II}-17* (data not shown). They also did not have increased nuclear number per OCL (Table 1). These results are consistent with our results from *p62*^{P392L}-transduced human OCL precursors and indicate that expression of *p62*^{P392L} induces a subset of pagetic characteristics, including hyperresponsivity to the osteoclastogenic cytokines RANKL and TNF-α, but does not result in development of OCLs that express the complete pagetic phenotype or development of pagetic-like lesions.

To further examine the mechanisms responsible for the increased levels of OCL formation in marrow cultures from TRAP-*p62*^{P392L} mice, we determined the time course for OCL formation, the rates of proliferation of OCL precursors and of OCL apoptosis, and the expression levels of OCL differentiation markers. As shown in Figure 6A, OCL formation in marrow cultures from TRAP-*p62*^{P392L}

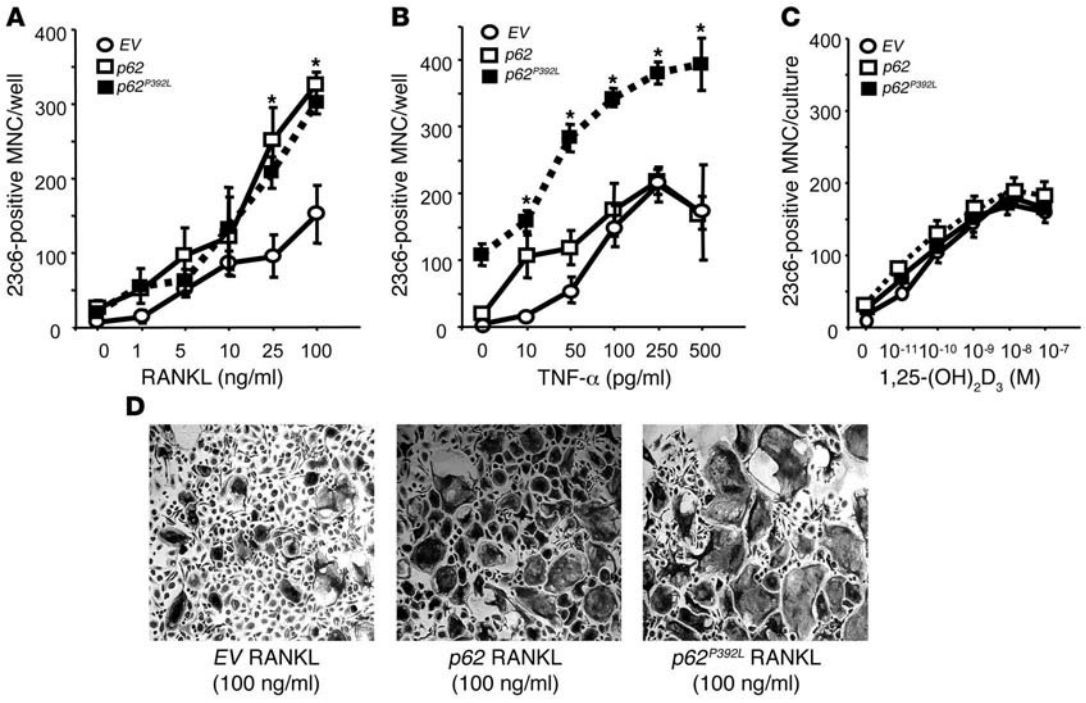

Figure 2
OCL formation by *p62*- and *p62*^{P392L}-transduced human OCL precursors. GM-CFU–derived cells (10^5 cells/well) transduced with *p62*, *p62*^{P392L}, or *EV* were cultured with RANKL (**A**), TNF-α (**B**), or 1,25-$(OH)_2D_3$ (**C**). After 3 weeks of culture, cells were fixed and stained with the 23c6 monoclonal antibody, which identifies OCLs. Results are expressed as the mean ± SEM for quadruplicate cultures from a typical experiment. *Significant differences ($P < 0.001$) compared with results of *EV*-transduced cell cultures treated with the same concentration of individual factors. A similar pattern of results was seen in 3 independent experiments. (**D**) Morphology of OCLs formed by *p62*^{P392L}- and *EV*-transduced GM-CFU–derived cells. Original magnification, ×100.

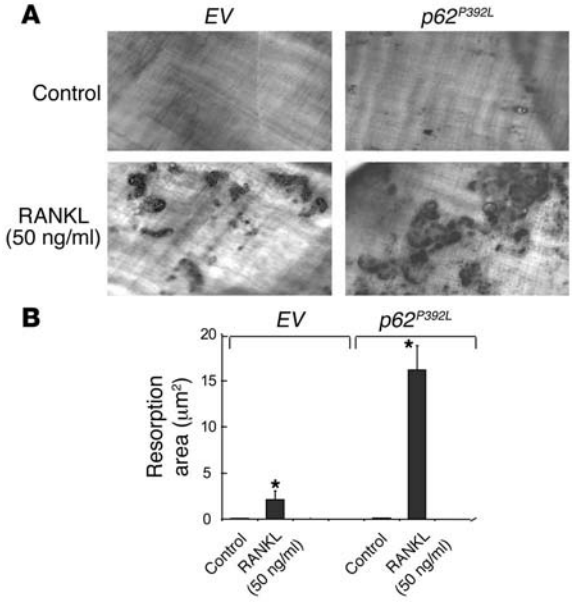

Figure 3
Resorption lacunae formed by OCLs from *p62^{P392L}*- and *EV*-transduced human GM-CFU. (**A**) Resorption lacunae formed on dentin by OCL. Original magnification, ×100. (**B**) Resorption areas per dentin slice for each treatment group. Results represent mean ± SEM for quadruplicate determinations for a typical experiment. Similar results were seen in 3 independent experiments. *Significant differences ($P < 0.05$).

mice was maximum after 6 days of culture while OCL formation in WT cultures was maximum at 9 days of culture. Further, OCL precursor proliferation was significantly increased in marrow cultures from *p62^{P392L}* mice compared with WT cultures but followed a similar time course (Figure 6B). In contrast, although the number of apoptotic OCLs was increased in TRAP-*p62^{P392L}* marrow cultures compared with WT marrow cultures, the percentages of apoptotic OCLs were similar (18% versus 10%; $P > 0.05$) in TRAP-*p62^{P392L}* and WT cultures after 9 days (Figure 6C). Apoptotic OCLs were not detected in cultures of mice from either genotype at day 3 or 6 of culture. Marrow cultures from TRAP-*p62^{P392L}* mice expressed relatively higher levels of TRAP, cathepsin K, and calcitonin receptor mRNA compared with WT cultures (Figure 7).

Since OCL precursors from Paget patients carrying the P392L mutation were hyperresponsive to 1,25-$(OH)_2D_3$ and also expressed *MVNP*, we transfected OCL precursors from TRAP-*p62^{P392L}* mice with *MVNP* and determined their responsivity to 1,25-$(OH)_2D_3$. As shown in Figure 8, OCL precursors from TRAP-*p62^{P392L}* mice transfected with *MVNP* were hyperresponsive to 1,25-$(OH)_2D_3$ and formed OCL at concentrations that were 1 to 2 logs lower than those of *EV*-transfected cells.

To further delineate the mechanisms responsible for the enhanced OCL formation in TRAP-*p62^{P392L}* mice, we examined inhibitor of NF-κB (IκB), p38 MAPK, and extracellular signal–regulated kinase 1/2 (ERK1/2) signaling in nonadherent marrow cells from WT and TRAP-*p62^{P392L}* mice. As shown in Supplemental Figure 2A, p-ERK1/2 was increased in marrow cells treated with RANKL or TNF-α while only modest changes were seen in p38 MAPK and p-IκB activity. Transfection of GM-CFU from WT and TRAP-*p62^{P392L}* mice with the MVNP gene further increased levels of NF-κB in TRAP-*p62^{P392L}* OCL precursors compared with those of WT precursors (Supplemental Figure 2B). Expression of MVNP in OCL precursors from WT or TRAP-*p62^{P392L}* mice did not increase expression of c-Fos.

Discussion

Mutations in the *p62* gene have been linked to PD in approximately one-third of patients with familial PD and a minority of patients with sporadic PD. However, it is unlikely that these mutations are sufficient to induce the OCL abnormalities and bone lesions that are characteristic of PD, since pagetic lesions are focal even in patients carrying germline *p62* mutations and some individuals harboring *p62* mutations fail to develop PD (11–13). To determine the role of *p62* mutation in PD, we characterized OCL precursors from familial PD patients carrying the most common PD-associated *p62* mutation (P392L) and compared them with normal OCL precursors. OCL precursors from *p62^{P392L}*-positive PD patients formed OCLs at lower concentrations of RANKL, TNF-α, and 1,25-$(OH)_2D_3$ than controls (Figure 1, A–C) and had increased TAF_{II}-17 expression (Figure 1D), all characteristic of PD; this was similar to our previous findings in OCL precursors from patients with sporadic PD (3–6). However, OCL precursors from these patients also expressed MVNP, which we have previously reported results in increased OCL formation in response to RANKL and 1,25-$(OH)_2D_3$ and to increased expression of *TAF_{II}-17* both in vitro and in vivo (6, 14).

To further characterize the contributions of *p62^{P392L}* to PD in the absence of *MVNP*, we transduced normal human OCL precursors with vectors encoding WT *p62* or *p62^{P392L}* or with *EV*. As with OCL precursors from PD patients, *p62^{P392L}*-transduced OCL precursors showed increased TNF-α and RANKL sensitivity (Figure 2, A and B) but, in contrast, did not demonstrate increased 1,25-$(OH)_2D_3$ responsivity (Figure 2C) or increased expression of *TAF_{II}-17* (Figure 4). In addition, nuclear number per OCL was not increased in *p62^{P392L}*-transduced OCLs (Table 1). Thus, these OCLs express only a subset of the characteristics of pagetic OCLs (15). Similar results were obtained when expression of the *p62^{P392L}* gene was targeted to cells in the OCL lineage in vivo. OCL precursors from TRAP-*p62^{P392L}* mice were hyperresponsive to RANKL and TNF-α but not to 1,25-$(OH)_2D_3$ (Figure 5, A–C) and did not express increased levels of *TAF_{II}-17*. Further, OCL formation in TRAP-*p62^{P392L}* mice was significantly increased in vivo by treatment with TNF-α (Figure 5, F and G).

Both RANKL and TNF-α activate signaling pathways involving p62 that ultimately lead to the activation of NF-κB, p38 MAPK, and ERK1/2, which are important for OCL formation and function.

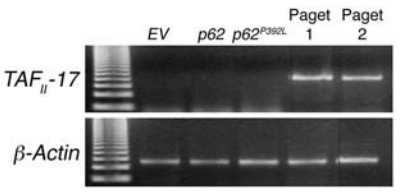

Figure 4
TAF_{II}-17 expression in *p62*-, *p62^{P392L}*-, and *EV*-transduced human OCL precursors.GM-CFU–derived cells (10^6 cells) transduced with *p62*, *p62^{P392L}*, and *EV* were cultured for 2 days with 10^{-8} M 1,25-$(OH)_2D_3$. RNA was then prepared and subjected to RT-PCR analysis of *TAF_{II}-17* or β-*actin* expression. The 2 PD patient samples shown in Figure 1 were used as positive controls.

Table 2
Cancellous bone structure and bone turnover in TRAP-*p62^{P392L}* mice

Variable	WT 4 mo	p62 4 mo	WT 8 mo	p62 8 mo	WT 12 mo	p62 12 mo	WT 16 mo	p62 16 mo
	n = 16	*n* = 9	*n* = 20	*n* = 11	*n* = 15	*n* = 3	*n* = 5	*n* = 11
F:M	14:2	7:2	15:5	6:5	13:2	3:0	3:2	1:10
BV/TV (%)	19.1 ± 0.8	15.4 ± 1.3[B]	15.3 ± 1.0	13.6 ± 0.7[B]	16.2 ± 1.1	11.5 ± 1.7[B]	17.6 ± 2.3	12.7 ± 1.0[B]
Tb.Wi (μ*m*)	36.6 ± 1.0	33.6 ± 0.9[B]	35.5 ± 1.3	32.9 ± 0.7[B]	39.0 ± 1.7	35.3 ± 3.7[B]	39.9 ± 3.3	32.2 ± 1.0[B]
Tb.N (per *mm*^{2})[C]	5.2 ± 0.2	4.5 ± 0.2[A]	4.3 ± 0.2	4.1 ± 0.2[A]	4.2 ± 0.3	3.2 ± 0.2[A]	4.4 ± 0.4	3.9 ± 0.3[A]
Tb.Sp (μ*m*)	158.2 ± 6.6	189.9 ± 10.1[A]	212.0 ± 14.0	216.0 ± 12.9[A]	214.8 ± 17.5	277.0 ± 22.6[A]	198.6 ± 29.1	235.6 ± 20.3[A]
Oc.Pm (%)	19.4 ± 0.8	22.7 ± 1.7[B]	18.0 ± 0.9	20.8 ± 2.0[B]	17.6 ± 0.7	27.4 ± 3.9[B]	16.8 ± 1.7	20.6 ± 2.3[B]
Ob.Pm (%)	12.3 ± 1.3	10.8 ± 1.6	8.4 ± 0.9[D]	7.4 ± 0.8[D]	8.8 ± 1.0[D]	4.5 ± 1.9[D]	8.9 ± 1.7[D]	13.0 ± 0.9[D]

Data are expressed as mean ± SEM. P62, TRAP-*p62^{P392L}* mice; BV/TV, cancellous bone volume; Tb.Wi, trabecular width; Tb.N, trabecular number; Tb.Sp, trabecular separation; Oc.Pm, OCL perimeter; and Ob.Pm, osteoblast perimeter. Data were analyzed using 2-way ANOVA. Significant differences are indicated as follows: [A]$P < 0.05$ and [B]$P < 0.01$ versus WT; [C]$P < 0.05$ and [D]$P < 0.01$ versus 4-month group. A significant interaction ($P < 0.05$) between the factors of treatment (*p62* or WT) and age (4, 8, 12, and 16 months) is noted in the variable of osteoblast perimeter.

Our results demonstrate elevated NF-κB activation as well as p38 MAPK and ERK1/2 signaling in OCLs expressing *p62^{P392L}*, strongly suggesting that Paget-associated mutations in p62 lead to increased osteoclastogenesis by stimulating signaling pathways that activate NF-κB (Supplemental Figure 2A). However, the detailed mechanisms by which these p62 mutations activate signaling remain to be determined. All of the PD-associated *p62* mutations reside in or near the ubiquitin-binding domain and result in loss of the ubiquitin-binding capacity of *p62* (16). Thus, it is possible that the ubiquitin-binding domain of *p62* normally mediates a protein/protein interaction that dampens NF-κB signaling in OCLs in response to inflammatory cytokines, such that loss of this interaction leads to increased activation of these pathways.

It is interesting to note that in both transduced human OCL precursors and in transgenic mouse OCL precursors, expression of *p62^{P392L}* had a much more dramatic effect on responsivity to TNF-α than to RANKL. Consistent with our results, Duran et al. have reported that the P392L mutation in *p62* increased NF-κB reporter activity (17). These results suggest that TNF-α, in addition to RANKL and 1,25-$(OH)_2D_3$, may be involved in the increased osteoclastogenesis in PD and should be studied further.

Histomorphometric analysis of vertebral cancellous bone in the TRAP-*p62^{P392L}* transgenic mice revealed a phenotype that was characterized by low bone volume with reduced trabecular number and width. OCL perimeter was increased at all ages examined, but there was no coupled increase in osteoblast perimeter. This marked imbalance between OCL formation and new bone formation is analogous to imbalance in inflammatory diseases of bone, such as rheumatoid arthritis and lytic bone metastases, in which bone formation is suppressed, rather than PD, in which OCL activity is closely coupled to new bone formation. This phenotype is very different from that observed in TRAP-*MVNP* transgenic mice, which persistently express the gene encoding the MVNP (14). In contrast with TRAP-*p62^{P392L}* mice, TRAP-*MVNP* mice displayed a bone phenotype that closely resembled PD in humans. This included a coupled increase in both bone resorption and new bone formation and enlarged OCLs with increased nuclear number (14). Moreover, a subset (30%) of 12-month-old TRAP-*MVNP* mice displayed pagetic-like lesions, with increased bone volume and dramatically thickened and disorganized trabeculae composed primarily of woven bone. No such lesions were observed in the TRAP-*p62^{P392L}* mice, which were examined up until 18 months of age. In addition, OCL precursors from the TRAP-*MVNP* mice showed increased sensitivity to 1,25-$(OH)_2D_3$ and expressed increased levels of *TAF$_{II}$-17*, findings that were not observed in the TRAP-*p62^{P392L}* mice unless the cells were transfected with *MVNP* (Figure 8). Finally, transfection of OCL precursors from TRAP-*p62^{P392L}* mice with *MVNP* further increased levels of NF-κB, suggesting that *MVNP* can increase the enhanced OCL formation induced by the *p62^{P392L}* mutation (Supplemental Figure 2B).

One possible explanation for the failure of the TRAP-*p62^{P392L}* mice to display increased osteoblast activity is that expression of *p62^{P392L}* is restricted to cells of the OCL lineage in this model while familial PD patients carrying a *p62* mutation express the mutant protein in all cell types. It remains to be determined whether the *p62* mutation plays a direct role in other cell types besides OCL in PD. It will therefore be of interest to evaluate the bone phenotype in knockin mice carrying the analogous *p62* mutation in the germline, which are currently being developed.

Taken together, these results demonstrate that the expression of *p62^{P392L}* in OCLs increases OCL formation but is not sufficient to induce PD. Thus, *p62* mutations may predispose to the development of PD by increasing basal OCL activity, but 1 or more additional factors are required for development of the full PD phenotype.

Methods

Chemicals. FBS was purchased from Invitrogen. All other chemicals and media were purchased from Sigma-Aldrich, unless otherwise noted. RANKL, TNF-α, IL-3, IL-6, and GM-CSF were purchased from R&D Systems. The 1,25-$(OH)_2D_3$ was generously provided by Teijing Corp. Polyclonal anti-IκBα, anti–p-IκBα, anti-p38, anti–p-p38, anti-ERK, and anti–p-ERK antibodies were from Cell Signaling Technology. Protease inhibitor mixtures and SB203580 were from Calbiochem.

Isolation of OCL precursors from PD patients carrying the p62^{P392L} mutation and from normal individuals. After obtaining informed consent, we obtained heparinized peripheral blood from 3 patients with PD and 3 age-matched controls. These studies were approved by the Institutional Review Boards at the University of Pittsburgh and the John Wayne Cancer Institute. Nonadherent peripheral blood mononuclear cells were isolated as previously described (18). The cells were cultured in methylcellulose in the presence of 100 pg/ml of recombinant human GM-CSF to form GM-CFU colonies. Individual colonies were pooled after 7 days of culture. Aliquots from the

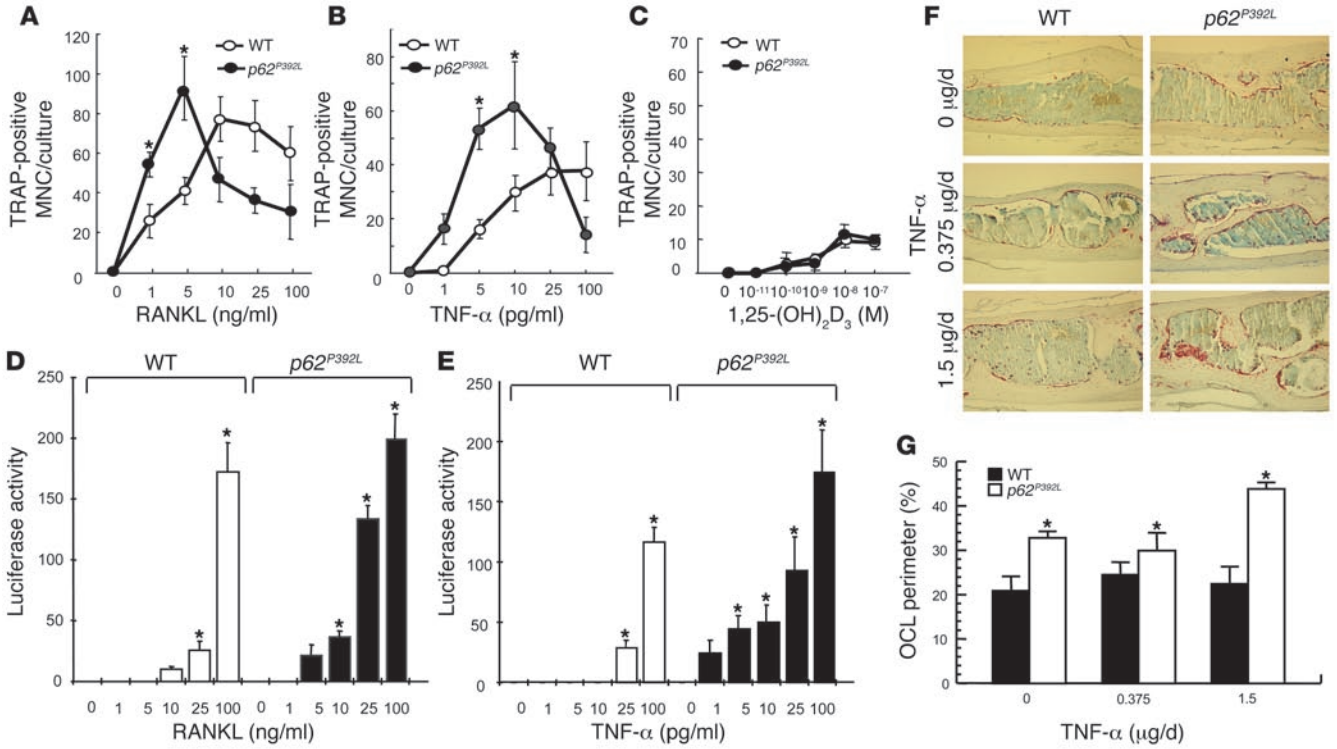

Figure 5

OCL formation and NF-κB gene reporter activity in OCL precursors from TRAP-*p62*^{P392L} and WT mice. (**A**–**C**) OCL precursors (10^5 cells/well) from TRAP-*p62*^{P392L} and WT mice were cultured in the presence of RANKL (**A**), TNF-α (**B**), or 1,25-$(OH)_2D_3$ (**C**). After 6 days of culture, cells were fixed and stained for TRAP activity. Results are expressed as mean ± SEM for quadruplicate cultures from a typical experiment. *$P < 0.001$ compared with results in WT cell cultures. Similar results were obtained in 5 independent experiments. Activation of NF-κB was measured by cotransfection of an NF-κB reporter plasmid and a β-gal expression vector into TRAP-*p62*^{P392L} or WT OCL precursors following 24 hours of treatment with RANKL (**D**) or TNF-α (**E**). The results are expressed as the mean ± SEM for the ratio of NF-κB reporter activity to β-gal activity for quadruplicate determinations. *Significant differences ($P < 0.001$) compared with results with WT cultures. A similar pattern of results was seen in 2 independent experiments. (**F**) Six-month-old TRAP-*p62*^{P392L} and WT mice were injected over the calvaria for 5 days with TNF-α (0, 0.375 μg, and 1.5 μg/day). Calvaria were harvested and tissue sections stained for TRAP activity (red color). Original magnification, ×100. (**G**) TRAP-positive OCL perimeter on the endosteal surface of calvaria in WT and TRAP-*p62*^{P392L} mice. *Significant differences ($P < 0.01$) between TRAP-*p62*^{P392L} and WT mice were found by 2-way ANOVA.

pooled colonies were cultured in the presence of RANKL, TNF-α, or 1,25-$(OH)_2D_3$ to induce OCL formation as described below.

Long-term cultures for OCL formation. For experiments employing highly purified OCL precursors, GM-CFU–derived cells, prepared as described above, were cultured in 96-well plates in α-MEM containing 20% horse serum and varying concentrations of RANKL, TNF-α, or 1,25-$(OH)_2D_3$. Every 3 days, half the medium was replaced, and after 21 days of culture, the cells were fixed with 1% formaldehyde and tested using a VECTASTAIN ABC-AP kit (Vector Laboratories) for cross-reactivity with the monoclonal antibody 23c6 (CD51), which recognizes the OCL vitronectin receptor. The 23c6-positive multinucleated cells were scored using an inverted microscope by an observer without knowledge of the treatment group.

Polymerase chain reaction amplification of RT-PCR. GM-CFU–derived cells were cultured for 2 days and subjected to RT-PCR analysis for expression of *MVNP* and *TAF*$_{II}$*17*. The gene-specific primers for human *MVNP* were 5′-CAGATTATGAACCAGTTTGGCCCTTCA-3′ (sense) and 5′-CCTGTGTTATTTCTTGGTTGTTTTCCC-3′ (antisense). The gene-specific primers for human *TAF*$_{II}$*17* were 5′-CATGCCATGGCTATGAACCAGTTTGGCCCCTCA-3′ (sense) and 5′-ATACTGCAGTTATTTCTTGGTTGTTTTCCG-3′ (antisense). The gene-specific primers for β-*actin* were 5′-GGCCGTACCACTGGCATCGTGATG-3′ (sense) and 5′-CTTGGCCGTCAGGCAGCTCGTAGC-3′ (antisense). Conditions for amplification were as follows: 94°C for 5 minutes, 35 cycles at 94°C for 1 minute, 55°C for 1 minute, and 72°C for 1 minute, followed by extension at 72°C for 7 minutes. PCR products were separated by 2% agarose gel electrophoresis and were visualized by ethidium bromide staining with ultraviolet light illumination (6).

Production of WT p62 and p62^{P392L} *vectors*. A plasmid containing the full-length human *p62* cDNA was kindly provided by J. Moscat (University of Cincinnati, Cincinnati, Ohio, USA), and the P392L mutation (a C-to-T transition) was introduced by PCR-based site-directed mutagenesis. The mutagenized cDNA was fully sequenced to verify correct introduction of the P392L mutation. Retroviral constructs containing the *p62* or *p62*^{P392L} cDNAs under the control of the CMV promoter were prepared and transfected into normal human OCL precursors as previously described (15). In brief, the *p62* or *p62*^{P392L} cDNAs were inserted into the *Xho*I site of the *p-LXSN* retroviral vector, and the recombinant plasmid constructs were transfected into the PT67 amphotropic packaging cell line using calcium phosphate. Stable cloned cell lines producing recombinant retrovirus at 10^6 virus particles/ml were established by selecting for resistance to neomycin (600 μg/ml). Similarly, a control retrovirus producer cell line was also established by transfecting the cells with the *p-LXSN EV*. Producer cell lines were maintained in DMEM containing 10% FBS, 100 U/ml streptomycin/penicillin, 4 mM L-glutamine,

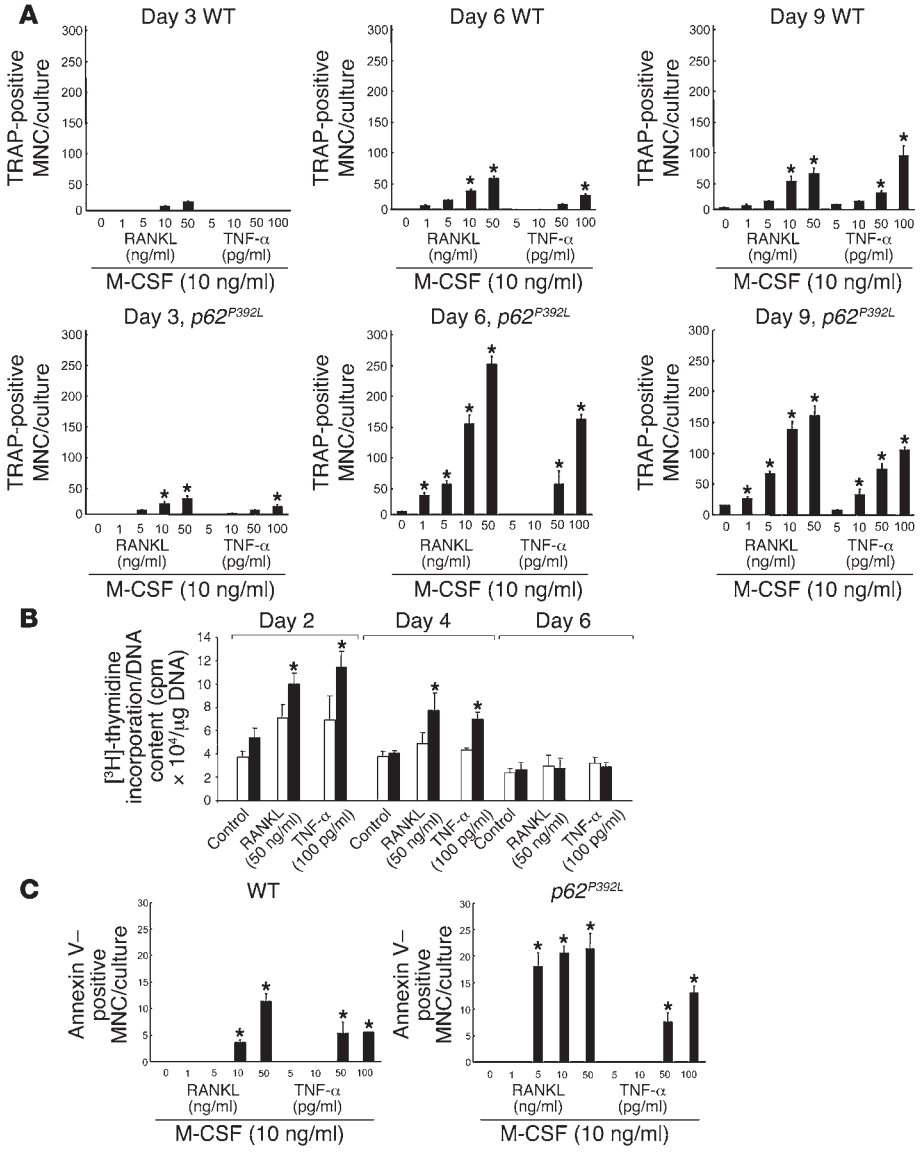

Figure 6
Time course for OCL formation, OCL precursor proliferation, and OCL apoptosis by marrow cells from TRAP-*p62*^{P392L} or WT mice. (**A**) OCL precursors (10^5 cells/well) from TRAP-*p62*^{P392L} and WT mice were cultured in the presence of RANKL or TNF-α. After 3, 6, or 9 days of culture, cells were fixed and number of TRAP-positive OCLs counted. (**B**) OCL precursors (1×10^6 per culture) from WT (white bars) and TRAP-*p62*^{P392L} (black bars) littermate mice were cultured for 2, 4, or 6 days and were pulsed at the end of the culture period for 1 hour with 1 mCi [^{3}H]-thymidine. Radioactivity was counted by liquid scintillation spectrometry. Results are expressed as the mean ± SD for quadruplicate cultures. *$P < 0.001$ compared with results of WT cultures treated with the same concentration of RANKL or TNF-α. (**C**) OCL precursors (10^5 cells/well) from TRAP-*p62*^{P392L} and WT mice were cultured in the presence of RANKL or TNF-α. After 9 days of culture, cells were fixed and number of apoptotic OCLs were counted using a commercial Annexin V kit (Promega). All results are expressed as the mean ± SD for quadruplicate cultures.

and high glucose (4.5 g/l). Retroviral supernatants from the producer cell cultures were collected and filtered (0.45 μm) for immediate use. The retrovirus stocks were demonstrated to be helper free by a marker assay. Viral titers present in the culture supernatants were determined by testing for multiplicity of infection with serial dilutions of the supernatants on NIH3T3 cells and scoring the number of G418-resistant CFUs formed (following exposure to 250 μg/ml G418) as described (15).

Overexpression of p62 and p62^{P392L} *in normal human OCL precursors*. After obtaining informed consent, we obtained bone marrow aspirates from normal volunteers as previously described (15). These studies were approved by the Institutional Review Board at the University of Pittsburgh. Human bone marrow mononuclear cells were cultured for 2 days in α-MEM containing 10% FBS and 10 ng/ml each of IL-3, IL-6, and SCF. The bone marrow cells were cultured for an additional 48 hours with varying amounts of viral supernatant (1–10% v/v) containing the *p62 or p62*^{P392L} vectors or *EV*. Cultures were supplemented with 4 μg/ml of polybrene, 20 ng/ml of IL-3, 50 ng/ml of IL-6, and 100 ng/ml of SCF. We previously determined that this was the optimum cytokine combination that supported the highest transduction efficiency. After 24 hours, cells were centrifuged, spent supernatant was removed, and freshly prepared viral supernatant supplemented with 4 μg/ml of polybrene and growth factors was added; then the cultures were continued for an additional 24 hours. After 48 hours, cells were harvested for short-term GM-CFU assays in methylcellulose as previously described (15, 19), and an aliquot of the cells was evaluated for p62 expression by immunostaining with an anti-p62 monoclonal antibody (BD Biosciences).

Bone resorption assays. GM-CFU–derived cells transduced with *p62*^{P392L} or *EV* (10^5 cells/well) were cultured with RANKL (50 ng/ml) or TNF-α (100 pg/ml) on mammoth dentin slices (Wako). After 3 weeks of culture, cells were removed, dentin slices were stained with acid hematoxylin, and areas of dentin resorption were determined using image analysis techniques, as previously described (20).

Construction of the TRAP-p62^{P392L} *hybrid transgene*. We have previously described construction of the p-BSmTRAP5′ plasmid, which contains 1294 bp of the 5′ flanking sequence as well as the entire 5′ untranslated region of the murine *TRAP* gene (21). The full-length human *p62*^{P392L} cDNA described above was inserted into the unique *EcoR*I site of *p-BSpKCR3* (21), which contains part of the second exon, the second intron, and the third exon, including the polyadenylation site of the rabbit β-globin gene. There are

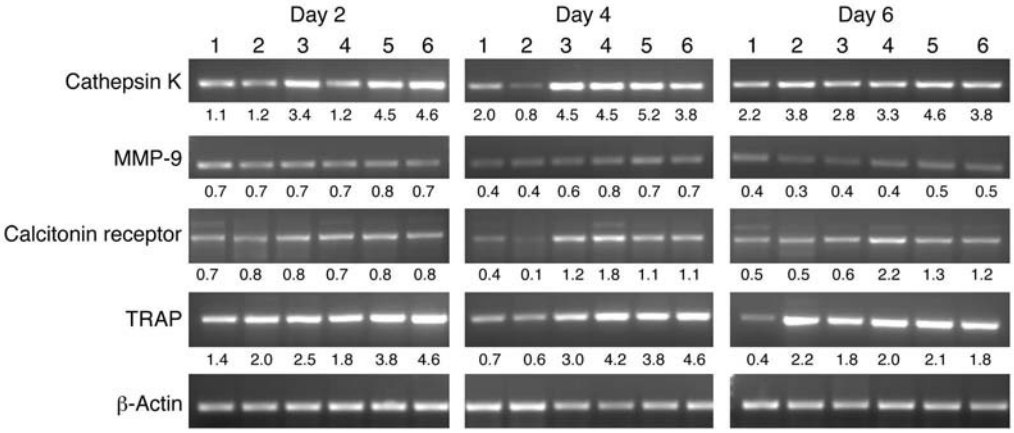

Figure 7
Expression of markers of OCL differentiation by TRAP-*p62*^{P392L} and WT OCL precursors. OCL precursors (10^6 cells) from WT and TRAP-*p62*^{P392L} littermates were cultured for 2, 4, or 6 days with 50 ng/ml of RANKL or 100 pg/ml TNF-α. RNA was prepared and subjected to RT-PCR analysis for cathepsin K, MMP-9, calcitonin receptor, and TRAP as described in Methods. Ratio of marker mRNA expression to β-*actin* is shown below each lane. Lane 1, WT M-CSF (10 ng/ml); lane 2, WT M-CSF (10 ng/ml) plus RANKL (50 ng/ml); lane 3, WT M-CSF (10 ng/ml) plus TNF-α (100 pg/ml); lane 4, *p62*^{P392L} M-CSF (10 ng/ml); lane 5, *p62*^{P392L} M-CSF (10 ng/ml) plus RANKL (50 ng/ml); lane 6, *p62*^{P392L} M-CSF (10 ng/ml) plus TNF-α (100 pg/ml).

no AUG initiation codons within the β-globin sequences upstream of the cDNA insertion site, so translation of the *p62*^{P392L} protein starts at the normal *p62* initiation codon. The murine TRAP promoter was then inserted into the multiple cloning site immediately upstream of the rabbit β-globin sequences. The *TRAP-p62*^{P392L} transgene was excised by XhoI digestion from the resulting plasmid, p–KCR3-TRAP-*p62*^{P392L}, and was agarose gel purified before microinjection.

Production and identification of TRAP-p62^{P392L} *transgenic mice*. These studies were approved by the Institutional Animal Care and Use Committee at Virginia Commonwealth University. The *TRAP-p62*^{P392L} transgene was microinjected at a concentration of 3 μg/ml into the male pronucleus of fertilized 1-cell mouse embryos by standard methods (22). The embryos were obtained from mating $CB6F_1$ (C57BL/6 × BALB/c) males and females (Harlan). The injected embryos were then reimplanted into the oviducts of pseudopregnant CD-1 female mice. The presence of the transgene was identified in resulting offspring by Southern blot analysis of genomic DNA prepared from a small tail-tip biopsy taken at the time of weaning. Probes for Southern blot analysis were generated by random oligonucleotide labeling (Amersham Biosciences) using [α-^{32}P] dCTP (DuPont/NEN). Transgenic mice of subsequent generations were identified by PCR analysis using transgene-specific primers. The upstream primer was derived from the murine TRAP5′ untranslated region: 5′-GTCCTCACCAGAGACTCTGAACTC-3′ (sense); and the downstream primer was derived from the human p62 cDNA: 5′-TGAGCGACGCCATAGCGAGCGG-3′ (antisense). The conditions for amplification were as follows: 94°C for 2 minutes, 35 cycles at 94°C for 1 minute, 60°C for 1 minute, and 72°C for 2 minutes, followed by extension at 72°C for 7 minutes. PCR products were separated by 1.25% agarose gel electrophoresis and were visualized by ethidium bromide staining with ultraviolet light illumination.

Histologic analysis of TRAP-p62^{P392L} *vertebral bones*. The first through fourth lumbar vertebrae from 4-, 8-, 12-, and 16-month-old *TRAP-p62*^{P392L} and WT littermates were fixed in 10% buffered formalin for 24–48 hours, then completely decalcified in 10% EDTA at 4°C, processed through graded alcohols, and embedded in paraffin. Longitudinal sections of 5 μm were cut and mounted on glass slides. Deparaffinized sections were stained for TRAP as described by Liu et al. (23). OCLs containing active TRAP were stained red. Another set of sections was stained with 0.1% toluidine blue. Histomorphometry was performed on the region of cancellous bone between the cranial and caudal growth plates of the third lumbar vertebral body under bright field and polarized light at a magnification of ×200, using the OsteoMeasure 4.00C morphometric program (OsteoMeasure; OsteoMetrics). OCL perimeter was defined as the length of bone surface covered with TRAP-positive and mono- and multinuclear cells. Osteoblast perimeter, cancellous bone volume, trabecular width, trabecular number, and trabecular separation were also quantified and calculated. All variables were expressed and calculated according to the recommendations of the American Society for Bone and Mineral Research Nomenclature Committee (24, 25).

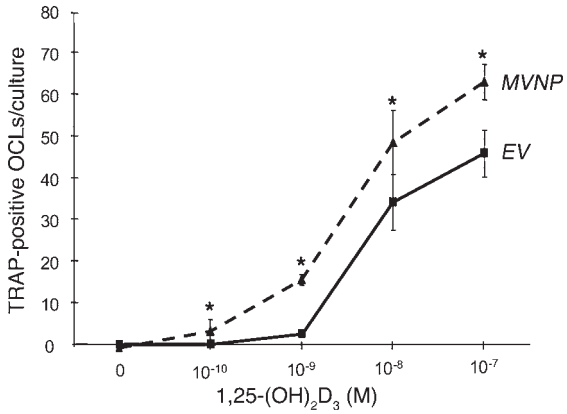

Figure 8
MVNP-transduced TRAP-*p62*^{P392L} mouse GM-CFU cells are hyperresponsive to 1,25-$(OH)_2D_3$. OCL precursors (5×10^5 cells/well) from *MVNP*- or *EV*-transduced TRAP-*p62*^{P392L} mouse GM-CFU were cultured in the presence of 1,25-$(OH)_2D_3$. After 9 days of culture, cells were fixed and stained for TRAP activity. Results are expressed as the mean ± SEM for quadruplicate cultures. *$P < 0.001$ compared with results of cultures of EV-transduced GM-CFU treated with the same concentration of 1,25-$(OH)_2D_3$.

NF-κB gene reporter activity in p62^{P392L} and WT marrow cells. For reporter gene assays, GM-CFU–derived cells from TRAP-*p62^{P392L}* mice or WT littermate controls were cotransfected with a luciferase reporter plasmid containing an NF-κB–responsive promoter (Clontech; Cambrex) and a β-gal expression plasmid using the FuGENE 6 Reagent (Roche Diagnostics). Sixteen hours after transfection, varying concentrations of RANKL or TNF-α were added. Twenty-four hours later, cells were harvested and lysed in the cell lysate solution provided with the luciferase assay kit (Promega). The luciferase activities of the cell lysates were measured with the luciferase assay kit according to the manufacturer's instructions and were normalized to β-gal activities of the same cell lysates using a β-gal assay kit (Promega).

Measurement of OCL differentiation markers in TRAP-p62^{P392L} and WT marrow cells by polymerase chain reaction amplification of RT-PCR. Marrow cells from TRAP-*p62^{P392L}* or WT mice were cultured for 2, 4, or 6 days with M-CSF (10 ng/ml) alone, RANKL (50 ng/ml) and M-CSF, or TNF-α (100 pg/ml) and M-CSF. Total RNA was extracted using RNAzol B solution (Tel-Test Inc.) and reverse transcribed as follows: 5% of the first-strand cDNA pool was subjected to PCR amplification using gene-specific PCR primers following standard PCR protocols. The gene-specific primers for mouse *cathepsin K* were 5′-GCAGAACGGAGGCATTGAC-3′ (sense) and 5′-TGGCTGGAATCACATCTTGG-3′ (antisense). The gene-specific primers for mouse *MMP-9* were 5′-TTGGTTTCTGCCCTAGTTAG-3′ (sense) and 5′-TGCCCAGGAAGACGAAGG-3′ (antisense). The gene-specific primers for mouse *calcitonin receptor* were 5′-CCCAGACATCCAGCAAGAG′ (sense) and 5′-CAGCACATCCAGCCATCC-3′ (antisense). The gene-specific primers for mouse *TRAP* were 5′-GAACTTCCCCAGCCCTTA-3′ (sense) and 5′-CCCACTCAGCACATAGCC-3′ (antisense). The gene-specific primers for mouse β-*actin* were 5′-GGCCGTACCACTGGCATCGTGATG-3′ (sense) and 5′-CCTGGCCGTCAGGCAGCTCGTAGC-3′ (antisense). The conditions for amplification were as follow: 94°C for 5 minutes, 35 cycles at 94°C for 1 minute, 55°C for 1 minute, and 72°C for 1 minute, followed by extension at 72°C for 7 minutes. PCR products were separated by 2% agarose gel electrophoresis and were visualized by ethidium bromide staining with ultraviolet light illumination.

Transduction of OCL precursors from TRAP-p62^{P392L} or WT mice with MVNP. Bone marrow cells were obtained by flushing the femurs of TRAP-*p62^{P392L}* or WT mice with α-MEM, and cells were collected by centrifugation at 300 *g* for 10 minutes. The cells were resuspended at 2.5×10^6 cells/ml and cultured in α-MEM containing 10 ng/ml each of IL-3, IL-6, and SCF for 2 days to induce proliferation of hematopoietic precursors. The marrow cells were then transduced with retroviral vectors that contained a neomycin resistance gene and the *MVNP* gene or *EV* (15). The transduced cells were cultured in methylcellulose with mouse GM-CSF (200 pg/ml) in the presence of 250 μg/ml G418 to select for GM-CFU colonies that expressed *MVNP* or *EV*. GM-CFU colonies were scored after 7 days of culture, using an inverted microscope. Colonies were individually picked, using finely drawn pipettes. GM-CFU–derived cells used for OCL formation assays are described below. We have previously demonstrated that these cells are highly purified early OCL precursors (15). GM-CFU–derived cells (10^6 cells /ml) obtained as described above (15) were plated in 96-well plates in α-MEM containing 10% FBS and cultured in the presence of 1,25-$(OH)_2D_3$ to induce OCL formation. The cultures were fed every 3 days by replacing half the medium, and after 6 days of culture, the cells were fixed with 1% formaldehyde and stained for TRAP using a leukocyte acid phosphatase kit (Sigma-Aldrich). The TRAP-positive multinucleated cells were scored using an inverted microscope.

Immunoblotting of OCL precursors from TRAP-p62^{P392L} or WT mice. Cytokine-treated or control OCL precursors from TRAP-*p62^{P392L}* or WT mice were washed twice with ice-cold PBS. Cells were lysed in the buffer containing 20 mM Tris, pH 7.5, 150 mM NaCl, 1 mM EDTA, 1 mM EGTA, 1% Triton X-100, 2.5 mM sodium pyrophosphate, 1 mM β-glycerophosphate, 1 mM Na_3VO_4, 1 mM NaF, and ×1 protease inhibitor mixture. Fifty micrograms of cell lysates were boiled in the presence of SDS sample buffer (0.5 M Tris-HCl, pH 6.8, 10% [w/v] SDS, 10% glycerol, 0.05% [w/v] bromphenol blue) for 5 minutes and subjected to electrophoresis on 7.5% SDS-PAGE. Proteins were transferred to nitrocellulose membranes using a semi-dry blotter (Bio-Rad) and incubated in blocking solution (5% nonfat dry milk in TBS containing 0.1% Tween-20) for 1 hour to reduce nonspecific binding. Membranes were then exposed to primary antibodies overnight at 4°C, washed 3 times, and incubated with secondary goat anti-mouse or rabbit IgG HRP–conjugated antibody for 1 hour. Membranes were washed extensively, and enhanced chemiluminescence detection assay was performed following the manufacturer's directions (Bio-Rad). All blots were densitometrically quantitated and the results expressed relative to control and normalized to β-*actin*.

Statistics. Significance was evaluated using a 2-tailed, unpaired Student's *t* test, with $P < 0.05$ considered to be significant.

Acknowledgments

This work was supported by research funds from the NIH grant PO1-AR049363 and US Army Medical Research & Materiel Command (USAMRMC) award DAMD17-03-1-0763 and is the result of work supported with resources and the use of facilities at the VA Pittsburgh Healthcare System, Research and Development. We acknowledge the General Clinical Research Center at the University of Pittsburgh for assistance with obtaining the marrow samples and the VCU Massey Cancer Center L.T. Christian III Transgenic Mouse Core Facility, which is supported by NIH grant P30-CA16059. J.J. Windle wishes to thank Heju Zhang and Christina Boykin for assistance with transgenic mouse production. H.E. Gruber wishes to thank Daisy Ridings for expert assistance with electron microscopy.

Received for publication February 17, 2006, and accepted in revised form November 13, 2006.

Address correspondence to: Noriyoshi Kurihara, VA Pittsburgh Healthcare System, Research and Development (151C-U), University Drive C, Pittsburgh, Pennsylvania 15240, USA. Phone: (412) 688-6000 ext. 81-4990; Fax: (412) 688-6960; E-mail: kuriharan@upmc.edu.

1. Tiegs, R.D., Lohse, C.M., Wollan, P.C., and Melton, L.J. 2000. Long-term trends in the incidence of Paget's disease of bone. *Bone*. **27**:423–427.
2. Siris, E.S. 1998. Paget's disease of bone. *J. Bone Miner. Res.* **13**:1061–1065.
3. Kukita, A., Chenu, C., McManus, L.M., Mundy, G.R., and Roodman, G.D. 1990. Atypical multinucleated cells form in long-term marrow cultures from patients with Paget's disease. *J. Clin. Invest.* **85**:1280–1286.
4. Menaa, C., et al. 2000. 1,25-Dihydroxyvitamin D_3 hypersensitivity of osteoclast precursors from patients with Paget's disease. *J. Bone Miner. Res.* **15**:228–236.
5. Neale, S.D., Smith, R., Wass, J.A., and Athanasou, N.A. 2000. Osteoclast differentiation from circulating mononuclear precursors in Paget's disease is hypersensitive to 1,25-dihydroxyvitamin D_3 and RANKL. *Bone*. **27**:409–416.
6. Kurihara, N., et al. 2004. Role of TAFII-17, a VDR binding protein, in the increased osteoclast formation in Paget's disease. *J. Bone Miner. Res.* **19**:1154–1164.
7. Laurin, N., Brown, J.P., Morissette, J., and Raymond, V. 2002. Recurrent mutation of the gene encoding sequestosome 1 (SQSTM1/p62) in Paget disease of bone. *Am. J. Hum. Genet.* **70**:1582–1588.
8. Hocking, L.J., et al. 2002. Domain-specific mutations in sequestosome 1 (SQSTM1) cause familial and sporadic Paget's disease. *Hum. Mol. Genet.* **11**:2735–2739.
9. Sanz, L., Sanchez, P., Lallena, M.J., Diaz-Meco, M.T., and Moscat, J. 1999. The interaction of p62 with RIP links the atypical PKCs to NF-kappaB activation. *EMBO J.* **18**:3044–3053.
10. Sanz, L., Diaz-Meco, M.T., Nakano, H., and Moscat, J.

2000. The atypical PKC-interacting protein p62 channels NF-kappaB activation by the IL-1-TRAF6 pathway. *EMBO J.* **19**:1576–1586.
11. Johnson-Pais, T.L., et al. 2003. Three novel mutations in SQSTM1 identified in familial Paget's disease of bone. *J. Bone Miner. Res.* **18**:1748–1753.
12. Falchetti, A., et al. 2005. Segregation of a M404V mutation of the p62/sequestosome 1 (p62/SQSTM1) gene with polyostotic Paget's disease of bone in an Italian family. *Arthritis Res. Ther.* **7**:R1289–R1295.
13. Singer, F.R., Lin, G., Hoon, D.S.B., Johnson-Pais, T.L., and Leach, R.J. 2004. Absence of evidence of Paget's disease of bone in subjects who harbor sequestosome 1 mutations [abstract]. *J. Bone Miner. Res.* **19**:M520.
14. Kurihara, N., et al. 2006. Expression of the measles virus nucleocapsid protein in osteoclasts in vivo induces Paget's disease-like bone lesions in mice. *J. Bone Miner. Res.* **21**:446–455.
15. Kurihara, N., Reddy, S.V., Menaa, C., Anderson, D., and Roodman, G.D. 2000. Osteoclasts expressing the measles virus nucleocapsid gene display a pagetic phenotype. *J. Clin. Invest.* **105**:607–614.
16. Cavey, J.R., et al. 2005. Loss of ubiquitin-binding associated with Paget's disease of bone p62 (SQSTM1) mutations. *J. Bone Miner. Res.* **20**:619–624.
17. Duran, A., et al. 2004. The atypical PCK-interacting protein p62 is an important mediator of RANK-activated osteoclastogenesis. *Dev. Cell.* **6**:303–309.
18. Kurihara, N., Chenu, C., Miller, M., Civin, C., and Roodman, G.D. 1990. Identification of committed mononuclear precursors for osteoclast-like cells formed in long term human marrow cultures. *Endocrinology.* **126**:2733–2741.
19. Kurihara, N., Civin, C., and Roodman, G.D. 1991. Osteotropic factor responsiveness of highly purified populations of early and late precursors for human multinucleated cells expressing the osteoclast phenotype. *J. Bone Miner. Res.* **6**:257–261.
20. Ishizuka, S., et al. 2005. (23S)-25-Dehydro-1{alpha}-hydroxyvitamin D3-26,23-lactone, a vitamin D receptor antagonist that inhibits osteoclast formation and bone resorption in bone marrow cultures from patients with Paget's disease. *Endocrinology.* **146**:2023–2030.
21. Reddy, S.V., et al. 1995. Characterization of the mouse tartrate-resistant acid phosphatase (TRAP) gene promoter. *J. Bone Miner. Res.* **10**:601–606.
22 Nagy, A., Gertsenstein, M., Vintersten, K., and Behringer, R. 2002. *Manipulating the mouse embryo: a laboratory manual.* 3rd edition. Cold Spring Harbor Laboratory Press. Cold Spring Harbor, New York, USA. 800 pp.
23. Liu, B., Yu, S.F., and Li, T.J. 2003. Multinucleated giant cells in various forms of giant cell containing lesions of the jaws express features of osteoclasts. *J. Oral Pathol. Med.* **32**:367–375.
24. American Society for Bone and Mineral Research President's Committee on Nomenclature. 2000. Proposed standard nomenclature for new tumor necrosis factor family members involved in the regulation of bone resorption. The American Society for Bone and Mineral Research President's Committee on Nomenclature. *J. Bone Miner. Res.* **15**:2293–2296.
25. Parfitt, A.M., et al. 1987. Bone histomorphometry: standardization of nomenclature symbols, and units. Report of the ASBMR Histomorphometry Nomenclature Committee. *J. Bone Miner. Res.* **2**:595–610.